Summer 2015

MyosinX is Required For Craniofacial Development in Danio Rerio

Cole Yancey

MYOSINX IS REQUIRED FOR CRANIOFACIAL DEVELOPMENT IN *DANIO RERIO*

by

COLE YANCEY

(Under the direction of Vinoth Sittaramane)

ABSTRACT

Craniofacial development is the process of laying early cartilage and bone patterns in the anterior region of the embryo, which ultimately results in shaping the structure of the face and head of an organism. Craniofacial abnormalities in humans, such as cleft lip and palate, are among the most common of all birth defects. Therefore, investigating the molecular mechanisms involved in craniofacial development will help us understand both evolutionary processes and genetic diseases. Craniofacial cartilage and bone structures are almost entirely derived from neural crest cells. Neural crest are a pluripotent migratory stream of cells that originate from the early developing brain and settle in final positions that give rise to the future skull and face. Several motor proteins are implicated in the migration of these neural crest cells. We have identified and isolated zebrafish *myosinX* mutants with defective craniofacial development. Currently, we are characterizing the role of *myosinX* in craniofacial development using various staining techniques. Alcian blue staining was used to identify specific defects within the cartilage, specifically ceratobranchial arches 3-5 are distorted or completely missing in *myosinX* deficient embryos. Using alizarin red staining techniques, pharyngeal tooth development was also examined. Tooth development occurs on the fifth ceratobranchial arch in a three crown clustered manner. However, in *myosinX* deficient zebrafish, pharyngeal crown protrusion was significantly hindered, showing only one developing crown within the tooth in most morphant embryos. This study used

immunohistochemical staining as well as RNA in situ hybridization techniques to identify the specification and position of migrating neural crest cells to establish a link between m*yosinX* and neural crest cell migration during early development. In *myoX* morphant and mutant individuals, craniofacial structures are significantly deformed compared to wildtype and control individuals. In addition, cranial neural crest cell migration is inhibited in *myoX* morphant and mutant individuals.

INDEX WORDS: Craniofacial, Myosin, Myo10, Myox, Myo10l1, Zebrafish, Cranial Neural Crest Cells, Cell Migration, Development

ABBREVIATIONS:

ATP - Adenosine Triphosphate
BCIP - 5-bromo-4-chloro-3'-indolyphosphate
BMP – Bone Morphogenic Protein
CNCC – Cranial Neural Crest Cell(s)
ENU - N-ethyl-N-nitrosourea (chemical formula $C_3H_7N_3O_2$)
FGF – Fibroblast Growth Factor
IB – Incubation Buffer
IQ Motif - "IQ" refers to the first two amino acids of the motif: isoleucine (commonly) and glutamine (invariably)
NBT - nitro-blue tetrazolium
NCC – Neural Crest Cell
PBS – Phosphate Buffered Solution
PBST - Phosphate Buffered Solution and Tween
PEST - proline (P), glutamic acid (E), serine (S), and threonine (T)
PFA - Paraformaldehyde
TMS - Tricaine mesylate

MYOSINX IS REQUIRED FOR CRANIOFACIAL DEVELOPMENT IN *DANIO RERIO*

by

COLE YANCEY

B.S., Creighton University, 2013

A Thesis Submitted to the Graduate Faculty of Georgia Southern University in

Partial Fulfillment of the Requirements for the Degree

MASTER OF SCIENCE

STATESBORO, GEORGIA

MYOSINX IS REQUIRED FOR CRANIOFACIAL DEVELOPMENT IN *DANIO RERIO*

By

COLE YANCEY

Major Professor:	Vinoth Sittaramane
Committee:	J. Scott Harrison
	Johanne Lewis

Electronic Version Approved:
Summer 2015

ACKNOWLEDGEMENTS

I would like to express my special appreciation and thanks to my advisor Dr. Vinoth Sittaramane, you have been a tremendous mentor for me. I would like to thank you for encouraging through this process and for allowing me to grow as a biologist. Your advice on both research as well as on my career have been priceless. I would like to thank Dr. J. S. Harrison and Dr. J. Lewis for serving as my committee members. A special thanks to all my fellow lab members who made spending countless hours in the lab a somewhat bearable experience. I would also like to thank all of my friends and family who supported me in writing, and incented me to strive towards my goal.

TABLE OF CONTENTS Page

LIST OF FIGURES Page

CHAPTER 1

INTRODUCTION

Vertebrate Craniofacial Development

The cellular and genetic events leading to the formation of the vertebrate skeleton begin early during the embryonic developmental process. In contrast to the vertebrae and limbs, where the skeleton is derived from mesoderm, cells of the neural crest play a pivotal role in this process in the head (Knight and Schilling, 2006). Neural crest cells must migrate out of the ectoderm to form the neurocranium and pharyngeal skeleton (Platt, 1893). The neurocranium (here referred to as the skull) protects the brain and sense organs while the pharyngeal skeleton, the jaws and gills, forms a muscularized pharynx for feeding and breathing (Hanken and Gross, 2006). The skull is an extremely complex and intricate structure. In humans, it comprises 22 separate bones as well as 20 deciduous and 32 permanent teeth. The boney skull structure is formed in two units; the neurocranium and the viscerocranium (Fig 1C). The *neurocranium is comprised of several b*oney interlocking plates that surround and protect the brain and sensory organs (Wilkie and Morris-Kay, 2001). The viscerocranium includes the bones of the face as well as the palatal, pharyngeal, temporal and auditory bones (Fig 1C). Craniofacial is a term which typically refers to the boney and cartilaginous structures of the skull and face, primarily located within the viscerocranium (Tapadia et al., 2005).

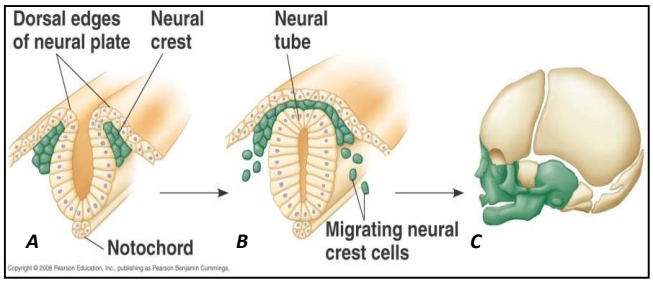

Fig 1.1: Neural plate folding to form the neural tube while neural crest cells migrate to one of many destinations. Highlighted in green are craniofacial structures and their precursor cells (Image modified from Pearson Education Inc.).

Experimental embryology has demonstrated that the neural crest cells that contribute to the cranial skeleton and connective tissues form the blueprint upon which the patterns of other tissues, such as muscles, are built (Noden, 1983). Thus, to understand cranial skeletal development, and head patterning in general, it is important to determine the intrinsic and extrinsic factors that control how neural crest cells are allocated to different fates. Craniofacial morphogenesis is a complex process which

provides the blueprint for building the vertebrate head and face. It is established very early during embryonic development and involves a multitude of precisely orchestrated temporal and spatial events. Even the slightest deviation from prescribed developmental events can cause catastrophic malformations. Craniofacial birth defects including cleft lip, cleft palate, small or absent facial and skull bones and improperly formed nose, eyes, ears, and teeth are present in one third of all children born with some sort of defect (Gorlin et al., 1990). A better understanding of the pathways and molecular mechanisms driving these processes could open up a new world of alternative MyoX plays an important role in CNCC migration (Sousa and Cheney, 2005) but it also has many other functions within the developing embryo. MyoX has been show to regulate netrin receptors and functions in axonal path-finding during neural development (Zhu et al., 2007). It has been shown to play an important role in filopodium formation by transportation of specific cargos within the cell (Liu et al., 2012). The nonsense mutation induced within out zebrafish model creates a premature stop codon which lies somewhere within the coil-coiled dimer structure of the MyoX motor protein. By truncating this region of the protein, we speculate that the FERM domains of the protein are not able to form properly, thus inhibiting any domain interactions between MyoX and its cargo/extracellular integrins (Wei et al. 2010).

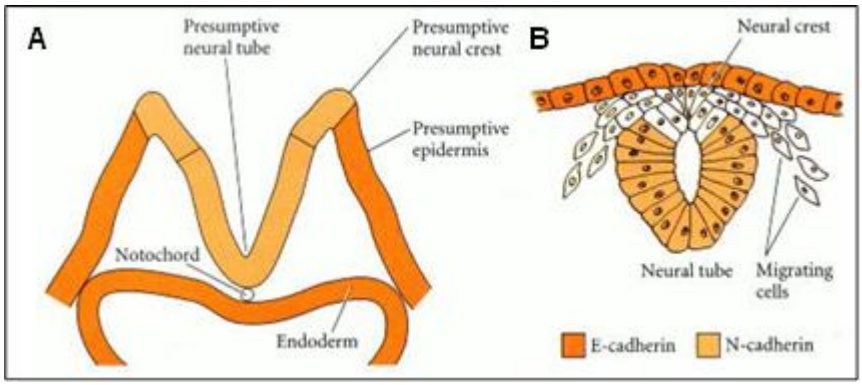

Fig 1.2: Localization of two different cadherins during the formation of the neural tube. (A) Schematic showing the folding of the presumptive epidermis into the neural crest with cadherin espression. (B) Schematic showing cadherin expressions in the epidermis, neural tube, and lack of cadherin expression in the neural crest resulting in budding neural crest cells. (Rutishauser et al., 1988)

In the early stages of embryonic development, specialized cell-types called the neural crest are formed at the junction between the neural plate and the non-neural ectoderm (Cordero et al., 2011), when the neural plate (Fig 1.1 A) rolls up and forms the hollow dorsal neural tube during neurulation (Fig 1.1 B). The neural tube eventually forms a closed cylinder that separates from the surface ectoderm. This separation is thought to be mediated by the expression of different cell adhesion molecules. Although

the cells that will become the neural tube originally express E-cadherin, they stop producing this protein as the neural tube forms, and instead synthesize N-cadherin and N-CAM (Figure 1.2 A) (Rutishauser *et al.,* 1988). As a result, the surface ectoderm and neural tube tissues no longer adhere to each other. Bone morphogenic proteins (BMP) 4 and 7 are two proteins that are known to be secreted by the presumptive epidermis (Liem et al. 1997). BMP4 and BMP7 induce the expression of the Slug protein and the RhoB protein in the cells destined to become neural crest along the dorsal side of the presumptive neural tube (Fig 1.2 B). If either of these proteins is inactivated or inhibited from forming, the neural crest cells fail to emigrate from the neural tube (Nieto et al. 1994).

All vertebrates share this derived characteristic of a neural crest made from the dorsal neural ectoderm. The 'neural crest' is a morphological term for the dorsal folds of the neural tube. The localization of neural crest precursors at the border between the neural plate and the epidermis suggests a potential for interactive signaling between the two tissues during induction of the neural crest (Klymkowsky et *al.* 2010). The vertebrate hindbrain is one key source of patterning information which exerts a profound influence on craniofacial development. During early vertebrate embryo development, the hindbrain becomes transiently subdivided into seven contiguous cell lineage restricted compartments called rhombomeres (r) (Fig 1.3A) (Vaage, 1969). Each rhombomere adopts a distinct set of molecular and cellular properties including restrictions in cell mixing and gives rise to unique regions of the mature adult brain (Marin and Puelles, 1995). The segmental organization of the hindbrain presages the establishment of an anatomical and functional registration between individual rhombomeres, cranial ganglia, branchiomotor nerves, and the migration pathways of cranial neural crest cells into the pharyngeal arches (Fig 1.3A) (Lumsden and Keynes, 1989). Rhombomeres

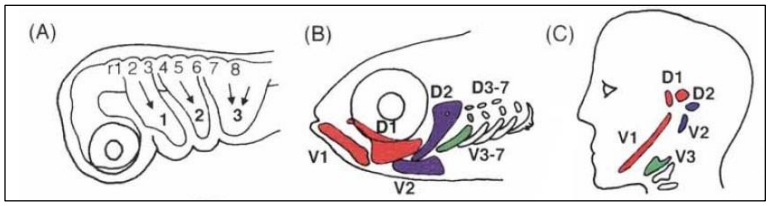

Fig 1.3: A comparison of different conserved craniofacial bones across varying species. All of the elements within a segment are coloured similarly: mandibular, 1 (red), hyoid, 2 (blue), first branchial, 3 (green), second through fifth branchials, 4-7 (white). (A) Migratory pathways of neural crest cells from rhombomeres to pharyngeal arches. (B) By larval and adult stages in the zebrafish. Each pharyngeal segment is further subdivided into dorsal and ventral skeletal elements. (C) Schematized, primitive pattern of a branchial arch (Schilling, 1997).

play an important role in housing the specification of cranial neural crest cells which then migrate ventrally to find their temporary resting position within the pharyngeal arches.

In all vertebrates, including humans (Fig 1.3 B-C), a series of pharyngeal arches develop along the lateral surface of the developing head region, which act as templates for the adult craniofacial structures. Once the cranial neural crest cells have aggregated within the pharyngeal arches, they will then migrate to their final destination within the developing embryo (Cordero et al., 2011). Typically the first arch, the jaw (mandibular), is supported by the second arch (hyoid, 2), and up to five more arches posteriorly (branchials, 3 to 7) develop gills in fishes or are incorporated into the throat in birds and mammals (Fig 1.3B) (Bronner, 2012). Teleost fishes retain what is thought to be the primitive skeletal pattern of ancestral gnathostomes (jawed vertebrates), including a large number of pharyngeal segments (seven in zebrafish), each with distinct dorsal and ventral elements. In all vertebrates, including humans, a series of pharyngeal arches develop along the lateral surface of the head. This homology makes zebrafish a powerful model for studying these developmental processes in human. In zebrafish, the pattern is most visible during the larval stages. During these stages, the pharyngeal skeleton develops first as cartilage but is subsequently replaced by endochondral bone, a process called endochondral ossification (Hanken and Hall, 1988).

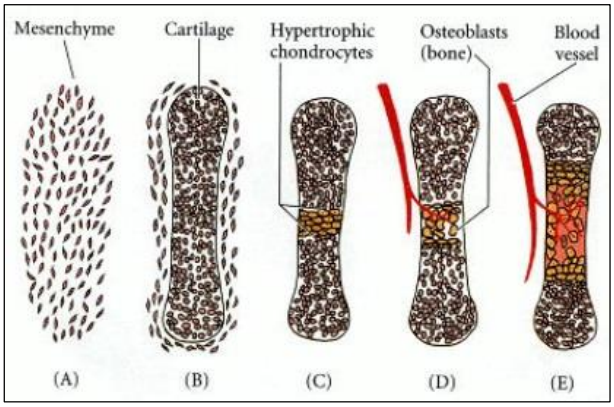

Fig 1.4: Different stages of endochondral ossification (Fayez et al., 2009).

Endochondral ossification involves the formation of cartilage tissue from aggregated mesynchymal cells, cranial neural crest cells for craniofacial development, and subsequent replacement of cartilage tissue by bone (Horton, 1990). The entire process can be broken down into five stages (Fig 1.4). First, mesynchymal cells are committed to become cartilage cells (Fig 1.4A). Nearby paracrine signals induce the expression of two distinct transcription factors within the mesynchymal cells, Pax1 and Scleraxis (Cserjesi et al., 1995). During the second stage, the committed mesynchymal

cells condense into compact nodules and differentiate into chondrocytes, cartilage cells (Fig 1.4B). Once these chondrocytes have formed, they proliferate extensively to form the cartilage model for bone formation. During the fourth phase, the chondrocytes stop dividing and increase their volume dramatically, becoming hypertrophic chondrocytes. These large chondrocytes alter the matrix they produce (by adding collagen X and more fibronectin) to enable it to become mineralized by calcium carbonate (Fig 1.4C). During the final phase of osterogensis, the cartilage model is invaded by surrounding blood vessels. The hypertrophic chondrocytes die by apoptosis and the space becomes bone marrow (Fig 1.4D-E). As these cells die, another group of cells that have surrounded the cartilage model differentiate into osteoblasts which begin forming bone matrix on the partially degraded cartilage (Bruder and Caplan, 1989) and eventually form bone structures. Thus, neural crest cell aggregation forms the underlying patterns that later become bone through the process of ossification. These cells are necessary to form the cartilage tissue that serves as a pattern for bone formation.

Neural Crest Cell Development

'Neural crest cells' are mesenchymal cells derived from the neural crest epithelium (Fig 1.1 B). The two most important characteristics of neural crest cells are their migratory ability as well as their multipotency (Donoghue et al. 2008). Neural crest cells shed away from the ectoderm, undergo an epithelial-to-mesenchymal transformation (Mishina and Snider, 2014), and migrate away from the future location of the brain and spinal cord. This transition gives rise to many different derivatives in the head and trunk regions.

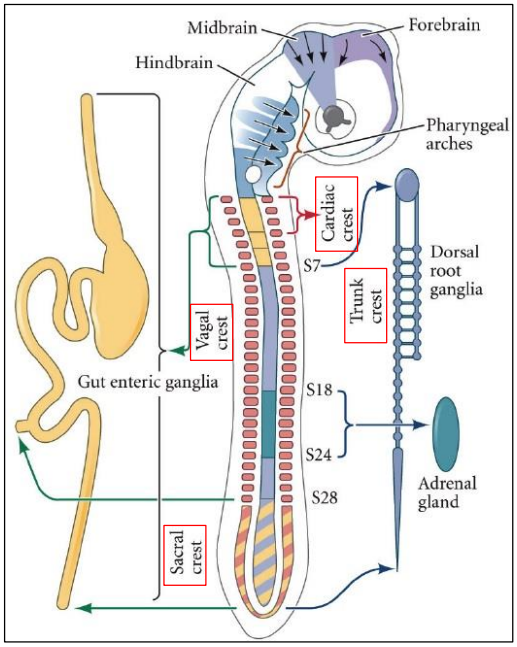

Fig 1.5: Neural crest cells throughout the developing embryo. Different neural crest regions are outlined with a box (Gilbert, 2000).

Neural crest-derived mesenchymal cells differentiate into at least 21 different cell types, including neurons (sensory, adrenergic and cholinergic); satellite, Schwann glial and chromaffin cells; melanocytes; connective tissue and skeletal cells (fibro-, chondro-,

osteo- and odontoblasts); myoblasts (cardiac, striated and smooth); adipocytes and angioblasts (Le Douarin & Kalcheim, 1999; Le Douarin et al. 2004; Vickaryous & Hall, 2006; Hall, 2009).

The neural crest can be divided into four main functional (but overlapping) domains: The cranial (cephalic) neural crest, the trunk neural crest, the vagal and sacral neural crest, and the cardiac neural crest (Fig 1.5). The cranial neural crest cells migrate dorsolaterally to produce the craniofacial mesenchyme that differentiates into the cartilage, bone, cranial neurons, glia, and connective tissues of the face. These cells enter the pharyngeal arches and pouches to give rise to thymic cells, odontoblasts of the tooth primordia, and the bones of middle ear and jaw. The trunk neural crest cells take one of two major pathways. The first pathway involves neural crest cells that become the pigment-synthesizing melanocytes. They migrate dorsolaterally into the ectoderm and continue on their way toward the ventral midline of the belly. The second migratory pathway takes the trunk neural crest cells ventrolaterally through the anterior half of each sclerotome. Sclerotomes are blocks of mesodermal cells, derived from somites, which will differentiate into the vertebral cartilage of the spine (Hall and Gillis, 2013). The trunk neural crest cells that remain in the sclerotome form the dorsal root ganglia containing the sensory neurons. These cells that continue more ventrally form the sympathetic ganglia, the adrenal medulla, and the nerve clusters surrounding the aorta.

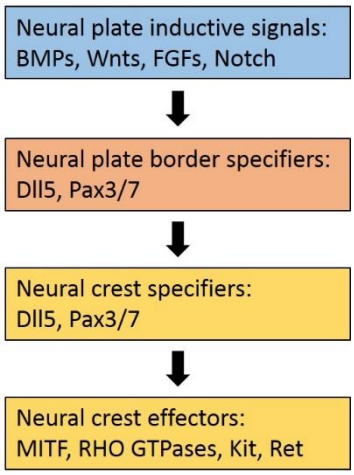

Fig 1.6: Molecular signals involved in each stage of cranial neural crest cell development.

The vagal and sacral neural crest cells generate the parasympathetic (enteric) ganglia of the gut (Le Douarin and Teillet 1973; Pomeranz et al. 1991). The vagal (neck) neural crest lies opposite vertebrate somites 1-7, while the sacral neural crest lies posterior to somite 28. Failure of neural crest cell migration from these regions to the colon results in the absence of enteric ganglia and thus to the absence of peristaltic movement in the bowels (Burns and Le Douarin, 1998). The cardiac neural crest is located between the cranial and trunk neural crests. In chick embryos, this neural crest region extends from the first to

the third somites, overlapping the anterior portion of the vagal neural crest (Kirby 1987; Kirby and Waldo 1990). The cardiac neural crest cells can develop into melanocytes, neurons, cartilage, and connective tissue (of the third, fourth, and sixth pharyngeal arches). In addition, this region of the neural crest produces the entire musculoconnective tissue wall of the large arteries as they arise from the heart, as well as contributing to the septum that separates the pulmonary circulation from the aorta (Le Lièvre and Le Douarin 1975). The focus of this study will be primarily cranial neural crest cells as facial cartilage and bone structures are derived from cranial neural crest cells only.

Cranial Neural Crest Cell Specification

In anamniotes such as *Xenopus* and zebrafish, neural-inducing bone morphogenic proteins (BMP) antagonists, such as Noggin and Chordin, generate a BMP signaling gradient that specifies dorsoventral patterning within the ectoderm. The neural plate border cell types form at intermediate levels of BMP signaling (Selleck et al., 1998). In Xenopus, partial inhibition of BMP signaling as well as activation of Wnt signaling mediates neural crest cell induction (Chang et a., 1998). Work in zebrafish also supports a role for both a BMP gradient and Wnts during neural crest cell specification (Fig 1.6). Also in Xenopus, fibroblast growth factor (FGF) signaling can induce neural crest in neuralized ectoderm, albeit through a Wnt intermediary, and seems to be a component of the neural crest-inducing signal from the paraxial mesoderm (Barth et al., 1999). Expression of FGF3, FGF4 and FGF8 has been observed in the paraxial mesoderm, although only FGF8 can induce a subset of neural crest markers in isolated Xenopus ectoderm without additional factors.

Foxd3 is an example of a gene whose expression is specific to neural crest precursors in the ectoderm of all vertebrates. It is weakly expressed in the paraxial mesoderm as well. Foxd3 gain-of-function expands the neural crest field and loss-of-function ablates neural crest precursors (Sasai et al., 2001). Foxd3 is expressed in undifferentiated embryonic stem cells, and is required for embryonic stem cell establishment and maintenance (Hanna et al., 2002). On the basis of their homology to linker histones, it has been postulated that winged-helix transcription factors like Foxd3

bind to nucleosomes and open compacted chromatin to potentiate transcription of target genes (Hanna et al., 2002). Indeed, a protein related to Foxd3, FoxA, has been shown to have such activity. So, Foxd3 might regulate the transcriptional accessibility of a collection of genes that are responsible for the multipotency of neural crest and other stem cells.

Cranial Neural Crest Cell Migration

Cranial neural crest cell (CNCC) migration can be broken down into three distinct phases (Fig 1.7). The initial phase of CNCC migration is defined by the acquisition of directed migration along the dorsolateral pathway. After CNCCs leave the hindbrain, they come into close contact with the surface ectoderm and cranial mesenchyme adjacent to the hindbrain. The second phase of CNCC migration involves the cells homing to the branchial arches. The cells move together in loosely connected streams along the dorsolateral pathway. The last phase of CNCC migration is entry into and invasion of the branchial arches (Kulesa et al., 2010). During the first phase, CNCC begin to leave the neural crest and join or start on a specific migratory pathway, depending on their beginning location within the neural tube and their migratory destination. CNCC morphologies vary depending on cell position within a migratory stream. CNCCs at the migratory front of a stream display protrusive activity in multiple directions, and trailing cells have a bipolar shape with equal leading and trailing edge protrusive activity aligned along the migratory route (Kasemeier-Kulesa et al., 2008). This enables the cells at the front of the migratory stream to lead the way while CNCCs with bipolar body shapes are able to make contacts with passing cells allowing them to follow along. The CNCCs within each particular stream communicate with one another by cell to cell contact. The cells also

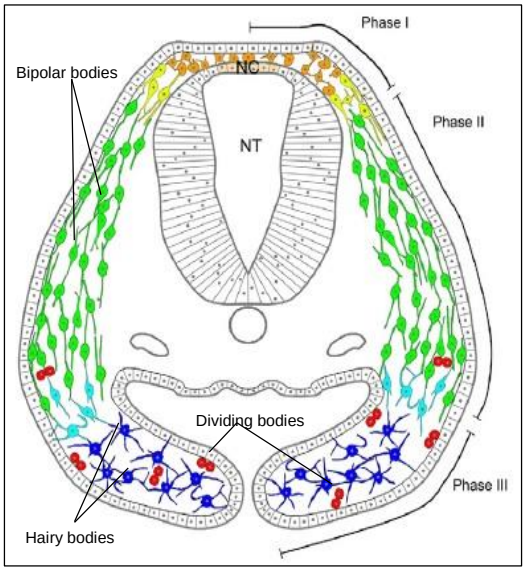

Fig 1.7: Cross section of a developing embryo illustrating the three phases of cranial neural crest cell migration as well as the different types of cell bodies. Neural crest, NC; Neural tube, NT (P.M. Kulesa et al., 2010).

project themselves forward using contact with the ectodermal wall. Cells require adhesive interactions with either each other and/ or extracellular substrates in order to actively migrate. During cell migration, cells first flatten and spread on the matrix to maximize their adhesions.

During the second phase, in which cells home towards the branchial/pharyngeal arches, CNCCs proliferate along their migratory route and this activity is key to the complete invasion of the branchial arches and formation of head and neck structures, as seen in figure 1.8. The proliferation of cranial NCCs appears to occur in a rigorous manner that involves the FGF/TGFbeta signaling pathways. Specifically, a subpopulation of CNCCs within the front portion of a typical migratory stream proliferates at a higher rate than the trailing cells (Kulesa et al, 2008). Higher cell proliferation within the migratory front may be triggered by space availability in the local environment as well as less physical limitations, in the form of cell crowding, on the front CNCCs. Leading CNCCs may in turn respond to molecular signals that stimulate proliferative activity causing them to move in a specific direction. Alternatively, lead CNCCs may contain an intrinsic mechanism that regulates their proliferative activity, regardless of microenvironmental signals or crowding around the cell.

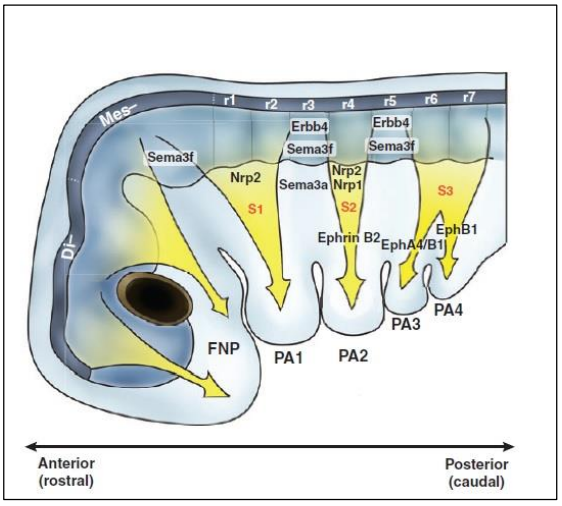

Fig 1.8: Migratory paths of cranial neural crest cells starting at the dorsal rhombomeres and finding their way into the specific pharyngeal arch (Minoux and Rijli, 2010).

There have been many proposed mechanisms to explain the migratory patterning and directionality of CNCC within the developing embryo. Contact inhibition of movement suggested that cells innately moved away from areas of dense cell populations (Abercrombie and Heaysman, 1953). However, the concept of cell nudging first introduced by Tickle and Trinkaus (1976) indicated that contact with neighboring cells can lead to forward movement. CNCCs would exert a mechanical influence on each other which causes membrane blebbing on the opposite side of the cell. Membrane blebbing would lead to lamellipodia protrusive activity and subsequent

directed cell movement. The leading model mechanism for CNCC directed movement involves receptor–ligand mediated guidance cues and the chemotactic response of cells to microenvironmental signals. CNCCs may respond to non-permissive cues present in the NCC-free zones (Farlie et al., 1999; Kulesa and Fraser, 1998). The points of contact between the cell and extracellular substrates and/or other cells are stabilized at the leading edge of the cell while the adhesion between the trailing edge and the matrix is released so that the cell body can be pulled forward.

After the CNCCs undergo their initial migration in the segmental streams, they must invade their target destinations and then properly assemble into differentiated structures. For example, the NCCs which came from the rhombomere 4 stream must invade branchial arch 2 (Fig 1.8) before they can form the facial bone and cartilage as well as any surrounding cranial ganglia. Recently it has been shown that this is not a passive event but rather a highly regulated one that involves multiple guidance cues including PCP signaling pathways and chemo attractant properties signaling of Fgfr1 and Nrp1 (Kulesa and Fraser, 1998) (Minoux and Rijli, 2010).

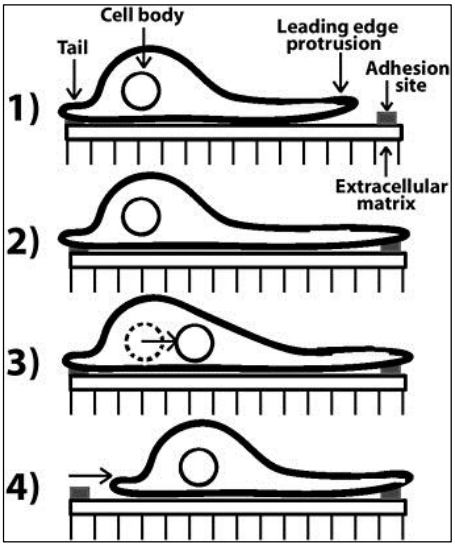

Fig 1.9: Schematic of how the cell migrates using cell-substrate adhesion and actin cytoskeletal mediated cell protrusions (Mofrad and Kamm, 2006).

The path taken by the migrating neural crest cells is controlled by extracellular matrices surrounding the neural tube (Newgreen and Gooday 1985). One set of proteins that promote migration include fibronectin, laminin, tenascin, various collagen molecules, and proteoglycans, and they are seen throughout the matrix encountered by the neural crest cells (Newgreen et al. 1986). Another set of proteins that impedes migration and provides the specificity for cellular movements are the ephrin proteins. These proteins are expressed in the posterior section of each sclerotome, and wherever they are, neural crest cells do not go (Krull et al. 1997). Eph receptors on the cellular surface of NCCs bind to the extracellular ephrin proteins and phosphorylate proteins within the NCC that interfere with the actin cytoskeleton that is critical for cell migration.

Motor Protein Mediated Cell Migration

In order for a cell to migrate towards its target properly, several variables must be properly aligned and functioning together. The process of cell migration begins with the extension of the cell surface in a particular direction. This protrusion generally occurs in response to chemoattractive signals in the microenvironment that are detected by the cell. The force required for protrusion to occur is propagated through the polymerization of the actin cytoskeleton. Actin filaments constitute the physical backbone of the cell protrusion as well as determining the overall shape of the cell. Actin filaments adopt a number of morphologies depending on the number of filaments in a given area of the cell and the number of actin binding proteins available. As a cell moves forward, the actin filaments bundle together within the protrusions to form structures such as filopodia, and lamellipodia (Fig 1.9). Filopodia are long, thin protrusions that emerge from the cellular membrane while lamellipodia are broad, sheet-like protrusions that contain a branched network of thin, short actin filaments. Once extended from the cell body, these protrusions must adhere to the extracellular substrate. The leading edge of the cell must then adhere to extracellular substrates while its tail is pulled forward due to cellular tension created by the leading protrusion. Motor proteins are an essential component for the intracellular communication that's necessary for cell protrusion and migration to occur.

The process of cranial neural crest cell migration is propagated by the use of specific motor proteins within the developing brain. Myosins are proteins that bind to actin filaments (F-actin) regulated by hydrolysis Adenosine triphosphate (ATP). Binding of F-actin promotes ATP hydrolysis by the myosin protein, which then powers the movement of actin filaments or allows the myosin to move along the actin filament itself. The 'motor' activity is enclosed within the N-terminal 'head' section of the myosin heavy chain. The C-terminal 'tails' of the heavy chains are largely atypical, binding to a varied array of proteins in the cell (Sokac and Bement, 2000). Myosins form over 30 distinct classes, based on sequence comparisons of the heavy chains (Richards and Smith, 2005). Traditionally, the first myosin class ever discovered, myosins-2, are considered 'conventional' and all other classes discovered afterwards are considered

‘unconventional’. The conventional myosins form large bipolar filaments via tail-directed homo-oligomerization (Fig 1.10). Unconventional myosins do not form filaments, although some have the ability to dimerize. Instead, their tails usually direct membrane binding and binding with other proteins.

The first myosin understood in detail was skeletal muscle myosin-2, which powers F-actin sliding in sarcomeres during muscle contraction (Lodish et al., 1995). Thus, when unconventional myosins were found to comprise the motor, fused to a variety of membrane-binding tails, it was naturally proposed that unconventional myosins function to move membranous organelles along actin filaments. This view spawned the ‘highways and local roads’ model in which microtubules serve as long range tracks for organelle transport powered by kinesins or dyneins, whereas F-actin serves as short range transport tracks powered by unconventional myosins (Langford, 1995). Once it became clear that some unconventional myosins were necessary for organelle trafficking, the idea gained considerable traction and has since then been included in both textbooks and primary cell biology literature (Lodish et al., 1995).

Many unconventional myosins carry membrane-enclosed organelles such as mitochondria, Golgi stacks, or secretory vesicles, to their correct locations in the cell. While conventional myosins cause cytoskeletal filaments to slide against each other which generate the force needed to produce muscle contraction, ciliary beating, and cell division. These myosin actin motors form complexes consisting of two heavy chains with motor heads and two light chains. These proteins associate with their filament tracks through a head region that binds and hydrolyzes ATP (Alberts et al., 2002). By coordinating their nucleotide hydrolysis cycle with conformational changes, the proteins cycle between states in which their head regions are tightly bound to the corresponding filament tracks and states in which they are unbound. Through this cycle of filament binding, conformational change, filament release, conformational relaxation, and filament rebinding, the motor protein and its associated cargo move one step at a time along the filament (typically a

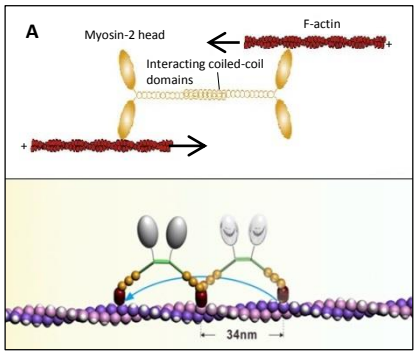

Fig 1.10: A) Conventional myosins interacting with an F-actin substrate during muscle contraction. B) unconventional myosins walking along a similar substrate bearing protein cargo (Lu et al., 2012).

distance of a few nanometers). The myosin tails have diversified during the process of evolution to permit dimerization of proteins with other subunits and to interact with different cargoes (Lu et al., 2012).

Unconventional Motor Protein Myosin X

Like all myosins, MyoX contains a motor domain that interacts with actin and hydrolyzes ATP. It contains several binding domains allowing for specific protein fastening. It contains three IQ motifs (The term "IQ" refers to the first two amino acids of the motif: isoleucine (commonly) and glutamine (invariably)) that allow calmodulin or calmodulin-like light chains to bind to the domain as well as a coiled-coil domain for dimerization. The tail of MyoX has a PEST region (a peptide sequence that is rich in proline (P), glutamic acid (E), serine (S), and threonine (T)) for proteolytic cleavage, three pleckstrin homology (PH) domains implicated in signaling through phosphatidylinositol phospholipids, and at the C-terminus, a myosin tail homology 4 (MyTH4) domain and a FERM domain (F for 4.1 protein, E for ezrin, R for radixin and M for moesin), important for binding microtubules and β-integrin (Sousa and Cheney, 2005). This structure suggests that MyoX may mediate membrane-cytoskeleton interactions. Studies in cultured mammalian cells show that MyoX is expressed at the edges of lamellipodia, membrane ruffles, and the tips of filopodia. Consistent with its location, MyoX is required for the formation and extension of filopodia. It not only induces the formation of filopodia by convergence of actin bundles through dimerization, but also promotes filopodial extension and stabilization by transporting integrin and actin binding proteins Mena/VASP to their tips (Berg and Cheney, 2002; Tokuo et al., 2007).

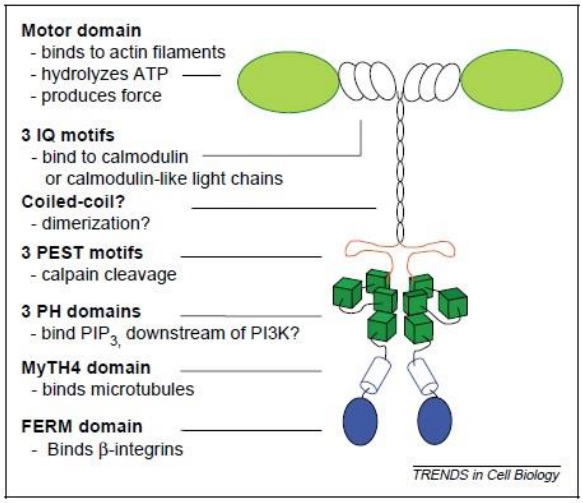

Fig 1.11: Model of myoX protein structure. Summarized domain structure and related function can be seen to the left. Although the myoX heavy chains are illustrated here as parallel dimers, their actual oligomerization status remains unclear. MyoX heavy chains might exist as stable monomers or dimers, undergo regulated dimerization, or form higher-order structures (Sousa and Cheney, 2005).

MyoX expression patterns have been previously characterized (Sittaramane and Chandrasekhar, 2008) and vary depending on location within the embryo as well as elapsed time after fertilization. At 18 hpf *myoX* is strongly expressed within rhombomere 5 and weakly expressed in rhombomeres 2, 3, and 4 (Sittaramane and Chandrasekhar, 2008). At 18 hpf, expression can also be seen within the hindbrain neurons, specifically within the trigeminal ganglion and lateral line ganglia by 30 hpf. During this same time frame, *myo10* is expressed within specific populations of cells of the forebrain and midbrain. In addition, *myoX* is expressed by the cells in the dorsal spinal cord by surrounding neural crest cells. These results suggest that *myoX*, among other myosins, are expressed in neurons and neural crest cells during the period of cell migration and specification (Sittaramane and Chandrasekhar, 2008).

In vitro culture experiments have suggested that *myosinX* is required for the adhesion of CNCCs to each other as well as the extracellular matrix. After knockdown experiments of *myoX*, neural crest cells attached but failed to spread on filopodia substrates, instead they remained round in shape (Nie et al., 2009). Filopodia are important membrane protrusive structures important for cell adhesion, movements and guidance. They sense the cell's surroundings and act as sites for signal transduction (Mattila and Lappalainen, 2008). Furthermore, *in vitro* results with Xenopus embryos suggest that *MyoX* is involved in maintaining contacts between neural crest cells. Knockdown of *MyoX in vivo* resulted in intermingling of neural crest cells between different branchial arch streams and abnormal migration patterns (Nie et al., 2009). Cadherins are transmembrane proteins which form adheren junctions binding cells within tissues together. They are a likely candidate for playing a crucial role in cell-cell adhesion during development since neural crest cells express different cadherins at different stages of migration. For example, in Xenopus, Cadherin 11 in turned on when CNCCs begin to migrate, indicating their possible role in CNCC migratory adhesion (Hadeball et al., 1998).

Like all myosins, MyoX contains a motor domain that interacts with actin and hydrolyzes ATP. It contains several binding domains allowing for specific protein fastening. Its domain structure suggests that MyoX may mediate membrane-cytoskeleton interactions in migrating cells (Berg and Cheney, 2002). *In vitro* culture

experiments have suggested that *myoX* is required for the adhesion of CNCCs to each other as well as the extracellular matrix. After knockdown experiments of *myoX*, neural crest cells attached but failed to spread on filopodia substrates, instead they remained round in shape (Nie et al., 2009). Previous results using Xenopus embryos suggest that *myoX* is involved in maintaining contacts between neural crest cells. Knockdown of *myoX in vivo* resulted in intermingling of neural crest cells between different branchial arch streams and abnormal migration patterns (Nie et al., 2009). The purpose of this study is to characterize the role of *myoX* with relation to craniofacial development and CNCC migration in zebrafish where it has never been previously identified.

Similar experiments have been conducted using Xenopus (Nie et al., 2009) however they must be done in zebrafish as well for several reasons. Zebrafish follow normal Mendelian inheritance rules as we understand them where Xenopus does not. Other models systems' (Xenopus included) gene expression is influenced by environmental factors during early embryogenesis. With zebrafish, we know that crossing two heterozygous individuals will results in 25% of the offspring expressing homozygous characteristics. Zebrafish have emerged as a great model system for studying development. It has many favorable characteristics which have contributed to its popularity as a model of disease in humans and developmental research; i.e. high fecundity, small size, rapid generation time, optical transparency during early embryogenesis. These characteristics have also contributed to its popularity to investigators in numerous other disciplines, including animal behavior, fish physiology, and aquatic toxicology (Lawrence, 2007).These valuable traits are extremely important when studying the genetic interactions seen in *myoX* dependent neural crest cells. Finally, the greatest advantage of using zebrafish is that these interactions can be visualized *in vivo* using fluorescent microscopy/imaging techniques.

Although *myoX* has been shown to be required for CNCC migration in *xenopus* (Hwang *et al.*, 2009; Nie *et al.*, 2009), very little is known about the localization and functions of *myoX* in CNCC destined to become craniofacial chondrocytes in zebrafish. In this study, I hypothesize that *myoX* is required for craniofacial development in *Danio rerio*. This study utilizes two different gene knockdown approaches to investigate the role of *myoX* in craniofacial development and CNCC migration. First, a strain of

zebrafish was acquired which contains a nonsense point mutation within the *myoX* gene. I also developed an anti-sense morpholino oligonucleotide to block MyoX protein production. Since *myoX* has been shown to be required for NCC migration in *xenopus*, and CNCC cells differentiate to become craniofacial chondrocytes, I used zebrafish to study the role of *myoX* in craniofacial development.

Because craniofacial bone development relies primarily on CNCC migration, CNCC migration in both mutant and morphant individuals was observed and characterized using both immunohistochemical staining as well as RNA in situ hybridization techniques. Based on the results found in the craniofacial cartilage characterization previously mentioned, I inferred that the migratory ability of the CNCCs was inhibited in *myoX* knockdown individuals. I hypothesize that *myoX* is required for CNCC migration in zebrafish as well. The goal of this study is to couple myoX motor protein activity to cranial neural crest cell migration with regards to craniofacial development in zebrafish.

CHAPTER 2

MATERIALS AND METHODS

Fish Strains

The zebrafish (*Danio rerio*) has recently emerged as a prominant vertebrate biomedical research model in many laboratories. The zebrafish strain myoXl1sa728 was used (zebrafish.org/zirc) in experiments as a model for genetic knock out fish and was acquired through the Zebrafish Mutation Project (Kettleborough et al., 2013). A mutagen, such as Ethylnitrosourea (ENU), is used to create hundreds of point mutations in male premeiotic germ cells. The sperm from these males are divided into two groups. One group is labeled and stored. The other group is analyzed to identify where the point mutations occurred. Once identified, the stored sperm cells can be used to create an F2 generation consisting of 50% wild type fish and 50% containing one copy of the mutated genome. When two heterozygous fish are bred, 25% of their offspring will be homozygous for the desired mutation.

Fish Husbandry

Adult zebrafish were maintained in a self-contained laboratory system following published materials (Westerfield, 2007). An IUCAC proposal has been submitted and approved for all research done in our lab using live zebrafish. Adult zebrafish are set up to breed using separate, smaller tanks and fertilized embryos are collected the morning after. Laboratory lights are automated in all fish laboratories to turn on at 9:00 A.M. and off at 11:00 P.M. This photoperiod 14 hours light and 10 hours dark are intended to simulate optimal natural breeding conditions. Fish are fed twice a day, once in the morning and once in the evening on a rotating fish feed cycle. A fish flake blend is fed in the morning while live brine shrimp are used to feed fish in the evening. Embryos were raised in tissue culture plates in 30% Danieu's medium at 28.5°C. To inhibit pigmentation in embryos to be viewed in whole-mount, 1-phenyl-2-thiourea (PTU, 0.003% final concentration) was added to the medium at approximately 15 hpf. Embryonic development is reported in actual hours or days post fertilization according to the published staging series (Kimmel et al., 1995).

Morpholino and RNA Rescue Injections

Glass needles were made in our lab using 3.5” Drummond replacement tubes (#3-000-203-g/x) in a Model P-1000 Fleming/Brown Micropipette Puller. Morpoholino powder provided from Gene Tools was resuspended in nuclease free water. Morpholinos are diluted in dextran tetramethyl-rhodamine and nuclease free water. Morpholinos must also be titrated to determine the lowest possible amount that is necessary to elicit a specific phenotype. The morpholino solution was then placed in the glass needle followed by oil to remove all the air within the needle. The tip of the needle must be broken to allow the flow of the morpholino using micro tweezers. Using a Nanoject II™ Auto-Nanoliter Injector, approximately 4.6 nl of the *myosinX* morpholino antisense oligonucleotide in a solution of 0.2% phenol red was injected into the yolk of 1–4 cell embryos. The translation start-site targeting *myosinX* MO, *myoXl1* (5’CCTCTGCGAAGAAGGTCTCCATCTT3’) was injected at 1.5 mg/ml. The concentrations reported were determined empirically to maximize effects on cartilage and teeth while minimizing general defects such as necrosis.

To assess the specificity of the MO knockdown, mRNA rescue experiment using the *myosinX* specific RNA was performed. Isolated zebrafish mRNA encoding the protein from the targeted locus is injected into the yolk of 1–2-cell embryos (Hyatt and Ekker 1999) and compared to MO injected embryos. RNA was prepared using an *in vitro* CAP RNA transcription reaction on the transcript of interest (myosinX). CAP RNA is a specially altered nucleotide on the 5′ end of some eukaryotic primary transcripts such as precursor messenger RNA. This process, known as mRNA capping (Fig 2.1), is highly regulated and vital in the creation of stable and mature messenger RNA able to undergo translation during protein synthesis. *MyosinX* cDNA was inserted into a pCS2+ plasmid vector and an *in vitro* synthesis reaction of

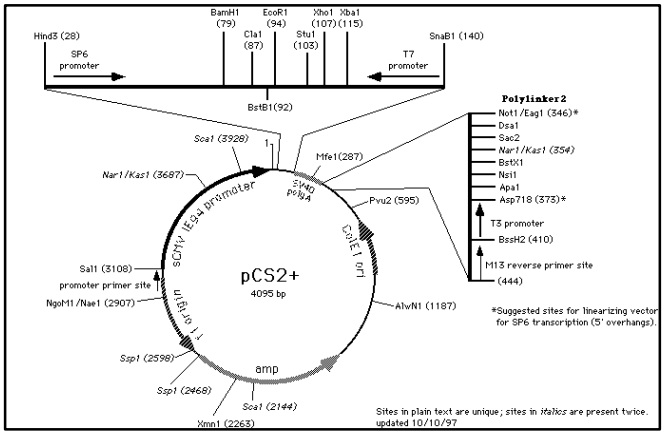

Fig 2.1*:* Vector map of pSC2+ vector. MyoX cDNA was inserted between BamHI and XbaI restriction enzyme sites.

large amounts of capped RNA was performed using mMessage mMachine SP6 kit (Ambion, Inc., AM1340). The RNA samples were then purified using the RNeasy Mini kit (Qiagen, Inc., 74104). Concentrations of RNA samples were then determined using a NANODrop 2000 spectrophotometer and stored at -80°C until ready for injections.

Genscript® and Subcloning

Subcloning was conducted using compotent E. Coli cells and agar medium. The pCS2+ vector was digested using ThermoScientific Fast Digest restriction enzymes (XbaI and BamHI). The *MyosinX* insert was isolated using specific primers and PCR, bands were separated using gel electrophoresis and extracted from the gel using a QIAquick Gel Extraction Kit. Upon successful ligation, plasmid/insert constructs were sent to the Sanger Sequencing Center at Clemson University for verification. A second method of construct synthesis was through the Genscript® biosynthesis company. The *myoX* gene was synthesized and subcloned into the psc2+ vector by Genscript®. The *myoX* sequence was provided to Genscript® (ENSDART00000113347) who constructed the synthetic (Fig. 2.2) insert and our lab provided the pCS2+ vector backbone for subcloning.

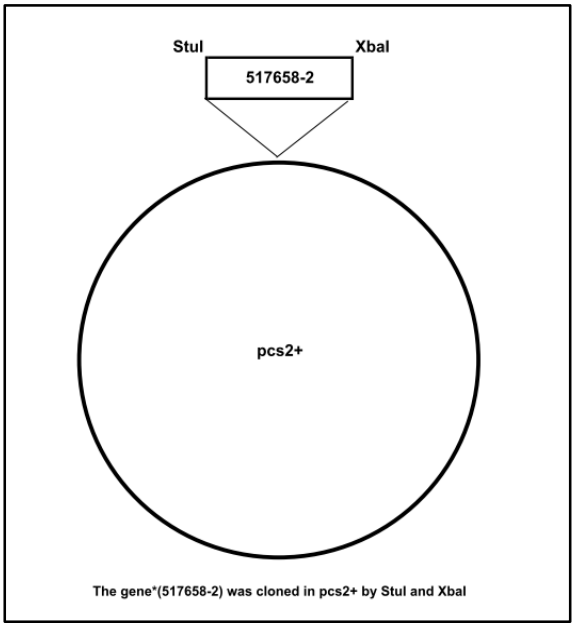

Fig 2.2*:* Vector map of pSC2+ vector and *myoX* insert as received from Genscript® MyoX cDNA was inserted between StuI and XbaI restriction enzyme sites.

To conduct rescue experiments, embryos are divided into several experimental groups—those injected with the targeting MO and with a control mRNA (i.e., GFP-encoding) versus those injected with the targeting MO and with the gene-specific mRNA, as well as mRNA constructs or MO alone (Brent et al., 2009).

Cartilage/Bone Staining and Immunohistochemistry

For cartilage preparations, the methods of Javidan and Schilling (2004) using alcian blue (Sigma) were followed, a dye that stains the extracellular matrix associated with chondrocytes. Larvae were anaesthetized using 200mg/L tricaine methanesulfonate (TMS) solutions at 6-6.5 dpf and tissues preserved in 4% neutral buffered formaldehyde (pH 7.0) at room temperature overnight. Pigmentation was removed by bleaching in 30% hydrogen peroxide for several hours to overnight and then transferred into a 0.01% solution of alcian blue dissolved in 70% ethanol/1% concentrated HCL. After staining in this solution overnight, embryos were rinsed in phosphate buffered saline with 0.1% Tween-20 (PBT) and rehydrated gradually into 70% glycerol solutions (embryos were exposed to 25% glycerol, then 50% glycerol first). Stained preparations were mounted in 70% glycerol.

To visualize pharyngeal tooth development, the two-color acid free bone and cartilage staining protocol of Walker and Kimmel (2007) was used. 100 mM $MgCl_2$ was used in place of acid to differentiate cartilage staining and limit tissue deterioration. An acid-free double stain solution was made in two parts that were mixed together just prior to staining. The first part includes alcian blue 8 GX (C.I. 58005, Sigma, St. Louis, MO) for cartilage staining and the second part includes alizarin red S (C.I. 74240, Sigma) for bone staining. The final concentrations for Part 1 are 0.02% alcian blue, 200 mM MgCl2, and 70% ethanol. Part 1 was made by first making a stock of 0.4% alcian blue in 70% ethanol. Because alcian blue is not readily soluble in 70% ethanol, the powder was added to a smaller volume of 50% ethanol, and occasionally mixed to dissolve; 100% ethanol and water were added to obtain final concentrations. 100 ml of Part 1 was made by adding together 5 ml 0.4% alcian blue in 70% ethanol, 70 ml 100% ethanol, and 100 mM $MgCl_2$ and water to obtain final concentrations. Part 2 is 0.5% alizarin red S powder dissolved in water. An acid-free double stain solution containing 10 ml of Part 2 and 1 ml of Part 1 was mixed just prior to staining. 6.5 dpf larvae were fixed and bleached in the same manner as in the alcian blue staining mentioned previously. 1 ml of acid-free double stain solution was added to larvae and rocked at room temperature overnight using a Fisher Scientific™ Platform Rocker. Stain solution was removed the following morning and tissue was cleared with successive changes of a solution of glycerol and KOH. After removing the staining solution, 1 ml of a solution of 20% glycerol and 0.25%

KOH was added and rocked at room temperature overnight. This solution was replaced by 1 ml 50% glycerol and 0.25% KOH and rocked at room temperature overnight.

To further increase bone and cartilage visualization, the methods of Javidan and Schiling (2004) for microdissections of stained cartilage were used, with few modifications. Using two Bioquip insect pins (No. 000) attached to the end of two Wilton Cookie Sticks with tape; the eyes were removed by gently pulling at the base of the socket and are discarded. One of the insect pins is bent to a 45° angle to be used as the securing pin while the other is left straight to be used as the dissecting pin. While securing the body of the larva with the securing pin, brain tissue was scrapped away anteriorly to posteriorly until little to none remains. Once eyes and brain tissue have been removed, the remaining yolk tissue was removed from the ventral side of the specimen in a similar manner to removing brain tissue. After positioning the securing needle, the dissecting needle was placed beneath the hyosymplectic (hs), near the joint between hs and the neurocranium and gently pulled to detach at the joint. This was repeated for the contralateral joint. The dissecting needle was then placed at the joint between the tip of the palatoquadrate (pq) and the ethmoid plate (ep) and gently pulled to detach. The dissecting needle was gently inserted horizontally, along the plane of the neurocranium and dorsal to the arches to remove any remaining soft tissue and repeated until the jaw and arches separate from the neurocranium. Neurocranium was then discarded while ventral structures are mounted in 70% glycerol and imaged using a Zeiss Stereo Discovery.V12 microscope with a mounted Axiocam Erc 5s and Zen Lite 2011 (Blue Edition) software at varying magnifications.

Immunohistochemical staining was done following the Zebrafish Fluorescent Antibody labeling protocol (Sittaramane, 2013). Embryos were fixed at various times post fertilization in 4% paraformaldehyde in phosphate buffered saline (PBS) solution. Embryos were washed 4 times in incubation buffer (IB) for 30 min per wash. Embryos were then washed in IB containing 1% horse serum for 30 min. After that wash, embryos were incubated overnight in IB with 1% horse serum and the proper diluted primary fluorescent antibody. Staining continued the next day with four 30 min washes in IB, an addition wash in IB containing 1% horse serum (30 min), and a final wash in IB containing 1% horse serum and the proper diluted secondary antibody. From this point

on, tubes containing embryos were wrapped in aluminum foil to protect fluorescent properties. On the final day of staining, the embryos were washed 3 times (5-10 min each) in 1X PBS and fixed in 4% paraformaldehyde overnight. Embryos were then washed in 1X PBS 3-4 times (5-10 min each) and progressively stored in 70% glycerol solution, stepwise.

RNA In Situ Hybridization

During RNA in situ hybridization, the utmost care was taken when handling the embryos and reagents during. All plastic ware and glassware was sterilized for at least 30 min prior to beginning to reduce the risk of contamination. Embryos were fixed in 4% paraformaldehyde/1XPBS (PFA-PBS) overnight and washed two times, 5 minutes each in PBS in the morning. A series of washes then took place in the following way: wash 1 X 5 min in 50% PBS/50% MeOH, wash 1 X 10 min in MeOH. Solutions were replaced with fresh MeOH and stored at -20°C overnight (minimum 2-3 hours). 100 ml PBS with Tween-20 was made using the following concentrations: 50 ml 2XPBS, 100 µl 100% Tween-20, 50 ml sterile H2O and used for a wash for 5 min in 50% MeOH/50% PBST. A second wash was performed for 5 min in 30% MeOH/70% PBST afterwards. The embryos were then washed twice for 5 min each in PBST. Embryos were fixed for 1 hour in PFA/PBS. Fix solution was removed and embryos were washed three times for 5 min in PBST each. Digest with 10 µg/ml Proteinase K in PBST (1 µl of 10 mg/ml Proteinase K + 999 µl PBST). Treatment times will vary with age--5 min for 20 hpf or younger, up to 20 min for 48 hpf or older embryos. Embryos were washed twice for 5 min each in PBST and fixed in PFA-PBS for 1 hour afterwards. Embryos were then washed three times for 5 min each in PBST and transferred after 2nd wash to 0.5 ml microfuge tube. Embryos were then washed one time for 10 min in 50% hyb/50% PBST and are ready for prehybridization preparation.

To prepare embryos for hybridization, embryos were incubated in 450 µl hybridization (hyb) buffer for at least two hours at 65°C on a rocking platform inside the incubator. 10 ml of hybridization buffer was made using the following reagents and volumes: 5 ml formamide, 2.5 ml 20XSSC, 10 µl of 50 mg/ml heparin, 500 µl of 10 mg/ml tRNA, 10 µl of 100% Tween –20, 1.888 ml DEPC'd water, 92 µl 1M citric acid

(pH~6.0). To perform hybridization, the prehybridization buffer was removed and 200 µl hybridization buffer with 100 ng of the specific probe was added to the tube. Typical probe concentration was 0.5 ng/µl. Tubes are then incubated overnight (9-12 hrs) at 65°C. The tubes are placed on a tilted platform (without rocking them) such that embryos are distributed along the wall of the tube. The used hybridization probe was then stored at -20°C and may be reused 2-3 times. The probe solution was then replaced with hybridization buffer and rinsed for 0.5-1 hour at 65°C.

Three washing solutions were made as follows; 10 ml Wash A: 1 ml 20XSSC, 4 ml ddH2O, 10 µl Tween, 5 ml formamide; 10ml Wash B: 1 ml 20XSSC, 9 ml ddH2O, 10 µl Tween; 10 ml Wash C: 1 ml Wash B, 9 ml ddH2O, 9 µl Tween. All washes were performed on a rocking platform. Embryos were washed using these solutions as described in the lab Sittaramane lab protocol and then incubated overnight at room temperature. The following morning, embryos were washed eight times for 15 min in Maleic Acid buffer containing 0.1% Tween. Immediately following, embryos were washed three times for 10 min in TMNT. Embryos were transfered to a 24 well microtiter plate after 2nd TMNT wash. TMNT was made using the following reagents and volumes: 5 ml 1M Tris-HCl, pH 9.5, 2.5 ml 1M MgCl2, 1.25 ml 4M NaCl, 50 µl 100% Tween-20, 41.15 ml sterile H2O, 50 µl 1M Levamisole.

To make Coloration solution, 45 µl NBT stock was added to 35 µl BCIP stock to 10 ml TMNT. 1 ml of coloration solution was used per well of embryos. Embryos were incubated at 37°C in the dark for 15 min-2 hrs, and watch for appearance of color in specific tissues. After color reaction was complete, embryos were washed 2-3 times rapidly with PBS and fixed overnight at 4°C in PFA-PBS. Embryos were brought to 70% glycerol gradually and were stored at 4°C indefinitely.

PCR and Sequencing

Genomic DNA was extracted according to the Meeker et al. 2007 protocol. Tissues were placed into microcentrifuge tubes containing 50 mM NaOH. The liquid volume used was sufficient for the complete submersion of the embryo (500ul). The samples were then heated to 95°C until the tissue was noticeably friable. 10 min was sufficient for fresh embryos and 20 min for paraformaldehyde-fixed embryos or adult

tissues. The tubes were cooled to 4°C, and then 1/10th the volume of 1 M Tris-HCL, pH 8, was added to neutralize the basic solution. The sample was centrifuged to pellet the debris, and the supernatant was immediately ready for use in PCR. One to 5 µl solutions were used per 25ul PCR.

PCR reactions are then set up using the aforementioned genomic DNA and *myosinX* specific forward and reverse primers designed specifically for this project (F: 5' CAT CAA ATA ACC ATT GGG AAA GTT CTT AAT 3', R: 5' TGT CAC TGA GCC ACG TAT GTG AAA CAA TGA 3'). The primers were designed to isolate and amplify the *myosinX* target sequence. PCR settings were run as follows: 1 cycle of 98°C for 5 minutes, 30 cycles of 98°C for 30 seconds, 55°C for 30 seconds, and 72 °C for 42 seconds, followed by 1 cycle of 72°C for 10 minutes and finally held at 4°C indefinitely. PCR products were verified using a 1% agarose gel electrophoresis protocol. Once the PCR products were confirmed, samples were sent to the Clemson University Genomics Center for Sanger Sequencing procedures.

Mutant Zebrafish Strain SA728

We obtained embryos containing a point mutation within the *myoX* gene from the Zebrafish Mutation Project (ZMP). Using a mutagen, such as Ethylnitrosourea (ENU), hundreds of point mutations are created throughout the genome and are outbred with wild type individuals to create strains of fish with single point mutations in each allelic portion of the genome (Kettleborough et al., 2013). This strain of zebrafish contains a single point mutation affecting amino acid number 805 (Fig 2.3 A). This point mutation changes the existing thymine to a

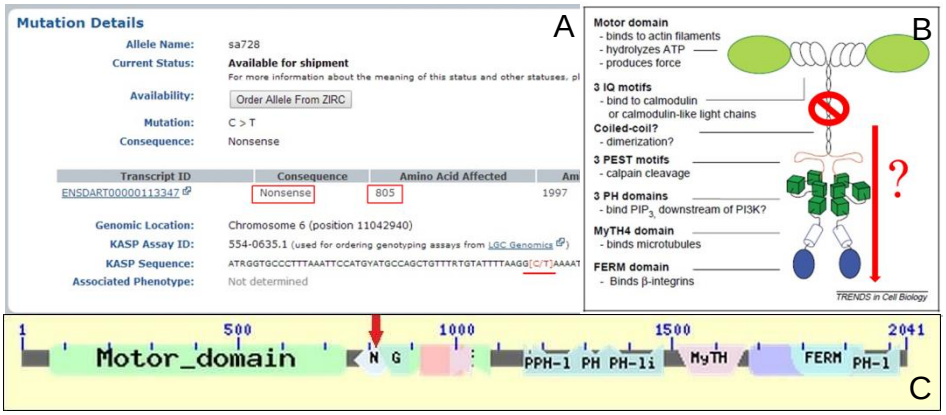

Fig 2.3 A) Mutation details regarding the SA728 zebrafish line provided by ZIRC. B) Map of the *myoX* genetic sequence and corresponding motor domains. C) Expected protein structure based on where the point mutation occurs within the sequence.

cysteine, causing a change in amino acid. It is hypothesized that this mutation disrupts the coiled-coil dimerization within the long arm of the myoX protein itself, according to the corresponding protein domain map (Fig. 2.3 B/C).

Cell Counts and Statistics

Alcian blue stained individuals were imaged using a Zeiss Discovery.V12 Stereo microscope and a Zeiss AX10 compound microscope. Cartilage cell counts were done using Zen 2011 Blue Edition and structure angles were measured using Zen 2011 Black Edition software. Cell shape analyses were done by outlining individual cells using Zen 2011 Blue software and measuring the cells at the longest and widest positions within each cell. Ratios between longest and widest points were compared between control and mutant individuals. Neural crest cell migration was visualized using sox-10 antibody marker and visualized using a Zeiss LSM 710 confocal microscope and processed using Zen 2011 Black Edition. Z stack images were compressed using maximum intensity image processing and cells were counted using ImageJ photo processing software.

Once uploaded into ImageJ, backgrounds were removed, image threshold was adjusted to remove noise produced from immunohistochemical staining, and particles larger than 20 pixels were analyzed. Each data set was collected from two different populations or from randomly selected individuals from the same population at different times and compared using a student's T test statistical analysis. Rescue experiments were analyzed using one way ANOVA statistical tests and compared individually using Tukey's test.

CHAPTER 3

RESULTS

MyosinX is Required for Craniofacial Development in Zebrafish

MyoX Mutant Individuals Display Craniofacial Deformities

Once grown, embryo morphology was compared between 138 wild type ($WT^{+/+}$) and 43 *myosinX* deficient ($myoX^{-/-}$) individuals from the same clutch (Fig 3.1). *MyoX* deficient zebrafish display shortened nasofrontal structures as well as a protruding lower jaw. The arrows highlight these abnormalities (Fig 3.1 A/B). The head region is much more flattened dorso-ventrally in *myoX* deficient individuals (Fig 3.1 A/B). Adult fish were positioned in the same manner and compared. Wild type zebrafish exhibit normal jaw structures while in the closed mouth position while the individual on the right to be *myoX* deficient based on its abnormal mouth formation (Fig 3.1 C/D). Approximately 25% of *myoX* mutant F2 offspring exhibit craniofacial deformities (45 individuals out of a total of 183 screened) (Fig 3.1 E). Zygosity of individuals was determined by examining external morphology only.

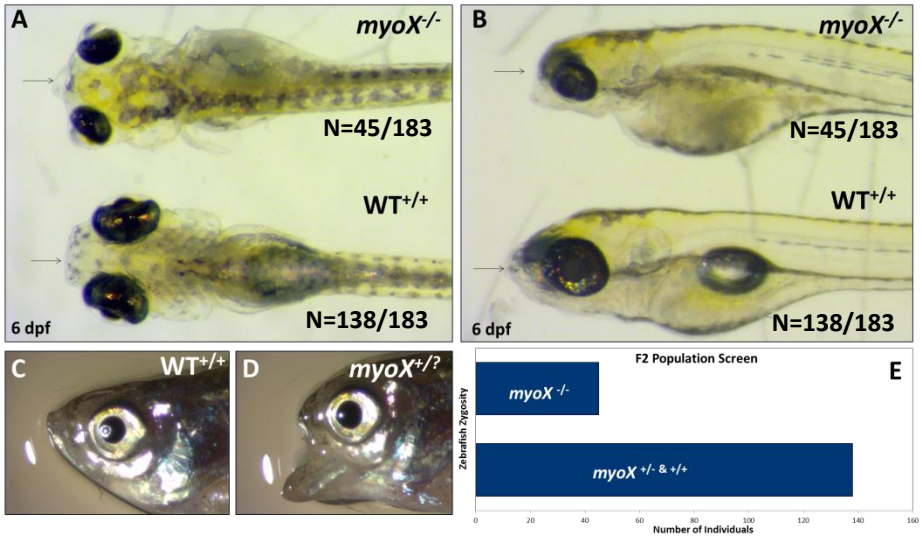

Fig. 3.1 Zebrafish morphology comparisons between 6 dpf mutant and wild type individuals as well as adult individuals. A) Dorsal view of Wild type whole embryos (top) versus mutant whole embryos (bottom). B) Lateral view of Wild type whole embryos (top) versus mutant whole embryos (bottom). C-D) Wild type adult zebrafish (left) and possible heterozygous mutant adult (right). E) Zebrafish zygosity from a batch of 183 siblings, 45 individuals show mutant phenotype.

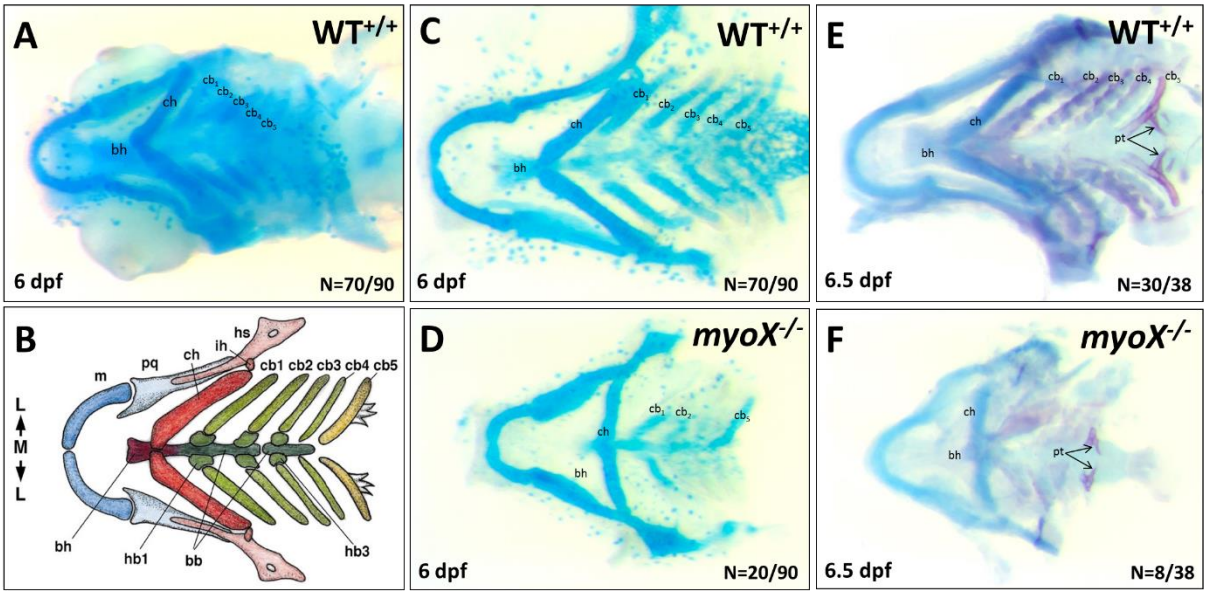

Fig 3.2 (A) Cartilage structures were stained using 0.01% Alcian blue. Visceral cranium in mutants shows developmental deformities as compared to wild type individuals. Abbreviations used: bb, basibranchial; bh, basihyal; cb, ceratobranchial; ch, ceratohyal; D, dorsal; hb, hypobranchial; hs, hyosymplectic; ih, interhyal; L, lateral; M, medial; m, Meckel's; pq, palatoquadrate; V, ventral.

Cartilage structures were stained using 0.01% Alcian blue solutions and visualized using a stereo microscope. Both the ceratobranchial (cb) arches as well as the basohyal (bh) structures were severely deformed in mutant fish. Ceratohyal (ch) formation displays an angle nearly 2x wider that which is seen in wild type zebrafish (mean wt angle = 63°, mean mutant angle = 36°). (Fig 3.2 C/D) To visualize cartilage development even further, previously stained structures were carefully dissected from the surrounding tissues. 20 fish showed the mutant phenotype out of 90 total (22%). By 6.5 dpf, pharyngeal tooth development can be visualized on the fifth ceratobranchial (cb) structure. A combination of Alcian blue and Alizarin red stains were used to simultaneously stain for bone and cartilage structures. 8 fish showed the mutant phenotype out of 38 total (21%) (Fig. 3.2 E/F). Pharyngeal teeth (pt) are underdeveloped in *myoX* deficient zebrafish.

Mutant and wild type cell shapes were measured and counted. Ceratohyal (ch) angle was measured as the angle of these structures largely determines the overall shape of the zebrafish face. Mutants CH structures were significantly shorter then in wild type individuals ($P<0.01$, $DF=18$, $t= 4.66$, $mean_{Mut}=13.9\mu m$, $mean_{WT}=21.8\mu m$, $SD=0.93, 1.44$) (Fig. 3.3 A/D/E). The distance from meckel's cartilage (m) to the neuro cranium (nc) as well as the distance from ceratohyal was measured as well as this was

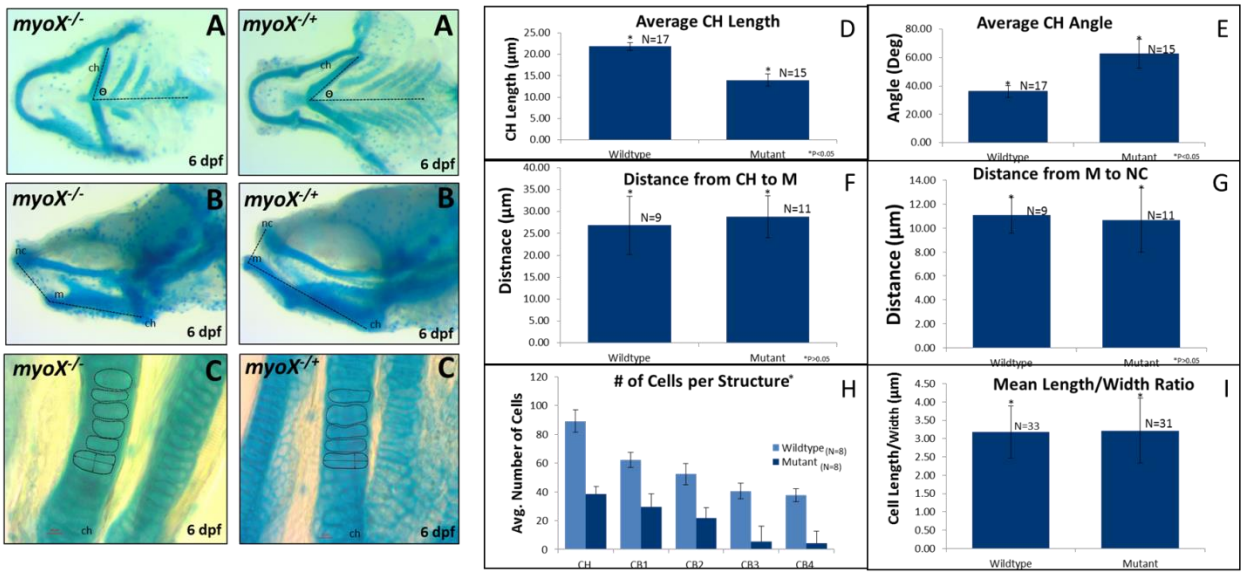

Fig. 3.3 Complete competency characterization of zebrafish cells in mutant and wild type individuals. A) Ceratohyal angle in mutant (left) versus wild type (right). B) Measurements from neural cranium to meckels cartilage to ceratohyal, lateral view, mutant (left versus wild type (right). C) Cell shape characterization in mutant (left) versus wild type (right). D-I) Graphs showing different cell characterizations. Bars indicate standard deviation.

a good indicator of facial dynamics. Mutant populations were not significantly different then wild type individuals (CH->M: P=0.46, DF=18, t=-0.75, $mean_{Mut}$=26.8µm, $mean_{WT}$=28.8µm, SD=6.6, 4.8) (M->NC: P=0.68, DF=18, t=-0.42, $mean_{Mut}$=10.6µm, $mean_{WT}$=11.1µm, SD=1.5, 2.7) (Fig 3.3 B/F/G). Individual cells were counted from the ceratohyal and ceratobranchial structures in both mutant and wild type individuals (Fig. 3.3 C). Wild type individuals had significantly more cells than mutant individuals in the ceratohyal structures (P<0.001, DF=14, t=-7.60, $mean_{Mut}$=38.4 cells, $mean_{WT}$=89.1 cells, SD=15.5, 10.8) and ceratobrachial (DF=14) (P_{cb1}<0.001, $mean_{mutcb1}$=29.7 cells $mean_{wtcb1}$=62.3 cells SD=10.6, 17.7, t_{cb1}=-4.47) (P_{cb2}<0.001 $mean_{mutcb2}$=21.6 cells $mean_{wtcb2}$=52.4 cells SD=14.7, 14.3, t_{cb2}=-4.25) (P_{cb3}=0.0022, $mean_{mutcb3}$=5.3 cells $mean_{wtcb3}$=40.5 cells SD=11.1, 21.8, t_{cb3}=4.08) (P_{cb4}<0.001, $mean_{mutcb4}$=4.3 cells $mean_{wtcb4}$=37.8 cells SD=8.7, 16.9, t_{cb4}=4.96) (Fig. 3.3 H). Cells were measured at their longest and widest points to determine shape. To determine cell shape, the ratio of length to width was compared between the two populations and no significant difference was found between populations (P=0.857, DF=62, t=0.18) (Fig 3.3 I)

MyoX Morphant Individuals Display Stunted Growth

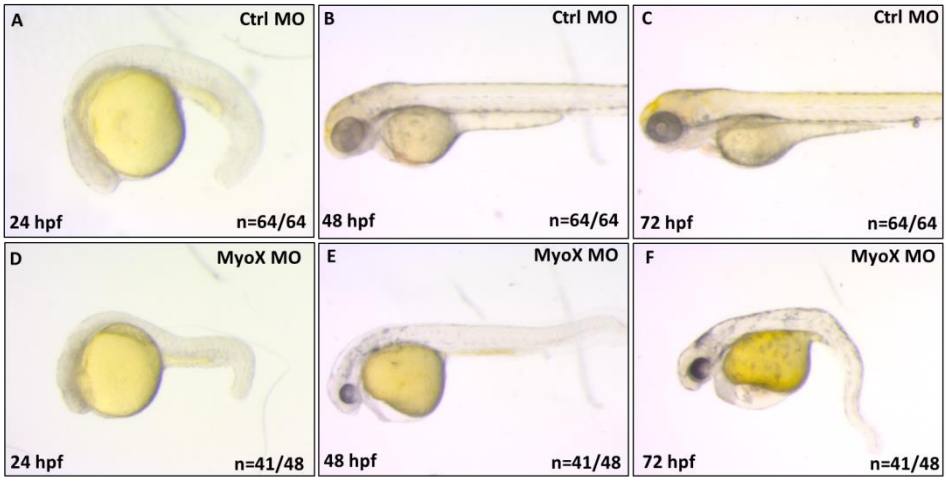

Fig 3.4 A/D) 24 hpf whole embryos, control (top) and *myoX* morphant individuals (bottom). B/E) 48 hpf whole embryos, control (top) and *myoX* morphant individuals (bottom). C/F) 72 hpf whole embryos, control (top) and *myoX* morphant individuals (bottom).

After injection of *myoX* morpholino, embryos were grown and preserved at specific time intervals to examine and compare embryo morphology. By comparing two separate knockdown techniques (morphant and mutant) we can better understand the mechanisms *myoX* is involved in. By 48 hpf, morphant embryos already exhibited distinct morphological differences than their control morpholino counterparts. 48 hpf morphants showed a delayed cranial development as well as curved or kinked tail structures (Fig 3.4 A/D). By 72 hpf, control embryo were beginning to swim on their own with a straight tail and diminished yolk. Morphant individuals at the same age displayed extremely curved/kinked tail structures as well as underdeveloped cranial structures including dwarfed size and abnormal shape (Fig 3.4 B/E). At 72 hpf, control individuals begin to form craniofacial structures

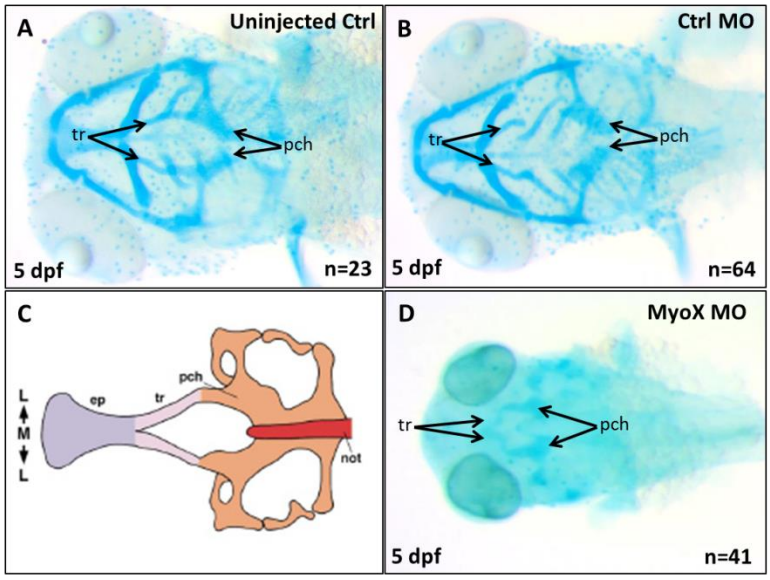

Fig 3.5 A) Uninjected control 5 dpf individuals. B) Control morphant individuals C) Diagram of wild type neuro cranium D) *MyoX* morphant individuals, dwarfed trabecula (tr) and parachordal (pch) structures.

while their face and head begins to flatten out. Morphants individuals' tails were completely curled underneath their bodies, while exhibiting cardiac edema. Morphant individuals were unable to swim at all and lacked any semblance of craniofacial structures when compared to control individuals (Fig 3.4 C/F).

MyoX Morphant Individuals Exhibit Stunted Cartilage Structures at 5 DPF

5 dpf embryos were stained using a 0.01% alcian blue solution to visualize craniofacial cartilage structures. Both control groups displayed well developed neurocranial structures as well as visceral cranial structures compared to expected craniofacial development (Fig 3.5 A-C). Morphant individuals displayed no signs of visceral cranium structures. These same individuals exhibited stunted growth in the neural cranium, specifically the parachodial and trabecular structures (Fig 3.5 D).

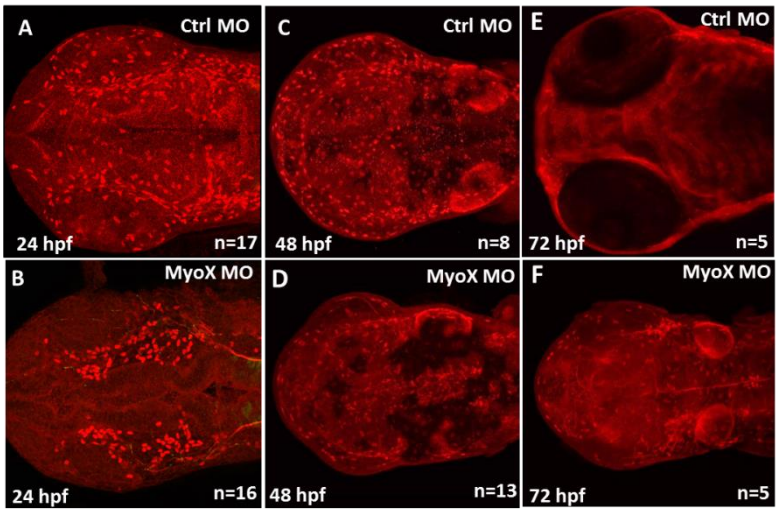

Fig 3.6 A-B) Control (top) and *myoX* morphant (bottom) 24 hpf individuals, sox-10 stained showing neural crest cell migration. C-D) Control (top) and *myoX* morphant (bottom) 48 hpf individuals. E-F) Control (top) and *myoX* morphant (bottom) 72 hpf individuals.

In conclusion, both morphant and mutant individuals exhibited disfigured craniofacial structures. In both groups, some amount of craniofacial cartilage was present but not in the sufficient amount to create full structures when compared to

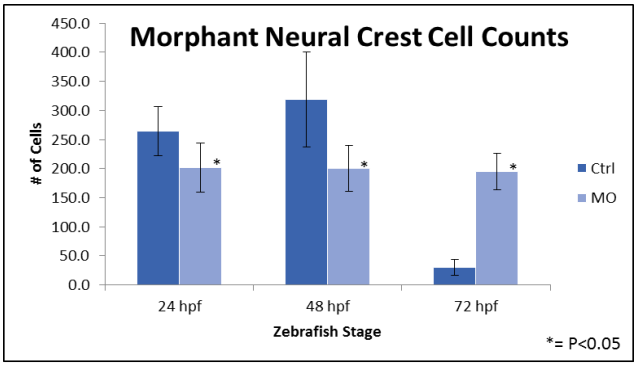

Fig 3.7 Sox-10 stained individuals were counted using ImageJ image processing software. All groups were significantly different. P_{24h}= 0.0002, P_{48h}= 0.004, P_{72h}=5.17E-06. Bars indicate standard deviation. Bars indicate standard deviation.

control groups. This indicates migratory inhibition in NCC as opposed to NCC specification being the root source of craniofacial structure disfiguration.

MyosinX is Required for CNCC Migration, Not Specification

Cranial Neural Crest Cell Migration Inhibited in *MyoX* Morphant Individuals

Cranial neural crest cell migration was visualized using immunohistochemical staining. Anti sox-10 anti-bodies were used to stain cranial neural crest cells at different stages of development in both control and *myoX* morpholino injected individuals. Once IHC staining was completed, cells were imaged using a Zeiss LSM 710 confocal microscope and processed using Zeiss Zen 2011 Black Edition software. 24 hpf control MO individuals displayed significantly more cranial neural crest cells than myoX morphant individuals (P= 0.0001, df=31, t= 4.24, $mean_{MO}$=201.7 cells, $mean_{CTRL}$=264.1 cells, SD=42.26, 42.15) (Fig 3.6 A-B, Fig 3.7). 48 hpf control individuals also displayed significantly more cells than there morphant counterparts (P=0.004, df=9, t=3.8, $mean_{MO}$=200.5 cells, $mean_{CTRL}$=318.6 cells, SD=82.19, 32.61) (Fig 3.6 C-D, Fig 3.7) However, 72 hpf control morphant individuals had significantly fewer cells than the 72 hpf *myoX* morphant individuals (P=5.17E-06, df=8, t=10.68, $mean_{MO}$=194.6 cells, $mean_{CTRL}$=30.2 cells, SD=13.52, 31.64) (Fig 3.6 D-E, Fig 3.7).

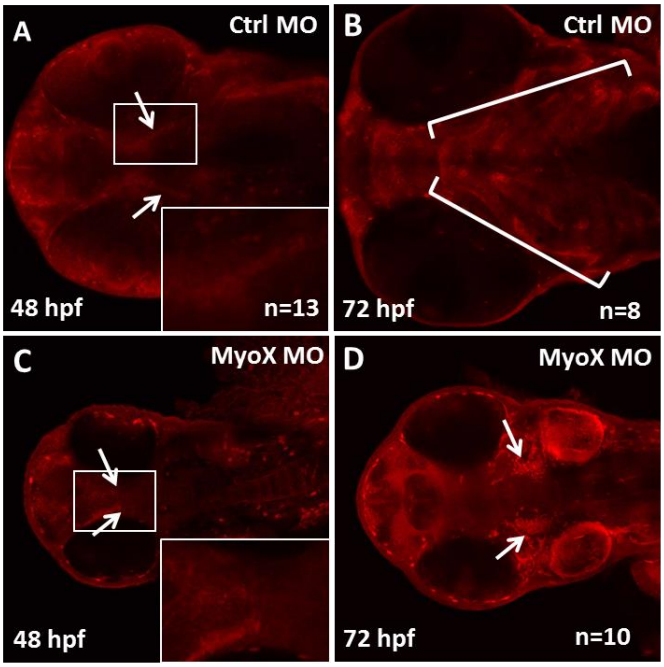

Fig 3.8 A-B) Control morphant 48hpf and 72 hpf individuals, sox-10 stained showing neural crest cell migration. C-D) *MyoX* morphant 48 hpf and 72 hpf individuals. Images shown are the bottom half of the embryos showing early craniofacial structure formation.

Early Craniofacial Structures Absent in *MyoX* Morphant Individuals

In addition to counting NCCs, visceral structures can be visualized starting from 48 hpf. This allows us to put the NCC count numbers into the developmental context of structure formation. Control individuals begin to form craniofacial structures at 48hpf (Fig 3.8 A) while morphant individual lack any organized craniofacial patterning (Fig 3.8 C). These cell aggregations form the underlying patterns for craniofacial bone structures in zebrafish. By 72hpf, control individuals show little to no NCC migratory

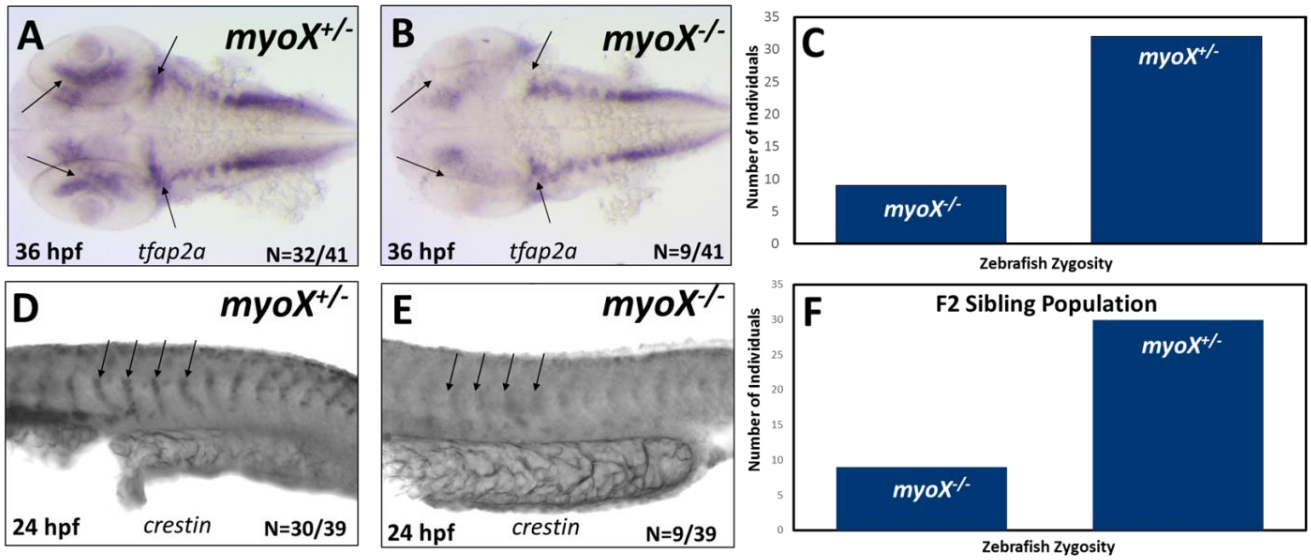

Fig. 3.9 A) In situ hybridization (tfap2) showing cranial neural crest cell migration in wild type zebrafish. B) In situ hybridization (tfap2) showing cranial neural crest cell migration in mutant zebrafish. C) 9 out of 41 (22%) total siblings exhibited the mutant phenotype. D) Migratory streams of neural crest cells in the tail of wild type individuals using in situ hybridization (crestin). E) Migratory streams of neural crest cells in the tail of mutant individuals using in situ hybridization (crestin). F) 9 out of 39 (23%) of the sibling population exhibit mutant phenotype.

cells (Fig 3.8 D) as structuring patterning is heavily underway (Fig 3.8 B). Groups of cells can be found in morphant individuals which resembles the same structures found during alcian blue staining at 5dpf.

In Situ Staining Shows Stunted NCC Migration in MyoX Mutants

In situ RNA hybridization (ISH) is a powerful tool in visualizing gene expression. By targeting genes expressed specifically in CNCCs, we can visualize their migration throughout the embryo. ISH was used to visualize neural crest cell migration in *myoX* mutant individuals. 41 siblings were stained with in situ hybridization using tfap2a and crestin riboprobes marking cranial neural crest cells (Fig 3.9 A-B). Heterozygous wild

type siblings exhibit wild type phenotypes while homozygous individuals show stunted neural crest cell migration as indicated by arrows (Fig 3.10 A-B). 9 of the 41 siblings exhibited mutant phenotypes (22%, Fig 3.9 C). 39 mutant siblings were hybridized using the crestin gene as a marker (Fig 3.9 D-E). Migrating streams of neural crest cells can be seen in the tail of wild type individuals (Fig 3.9 D), indicated by arrows, while the same streams of cells are not present in mutant individuals (Fig 3.9 E). 9 out of 31 mutant F2 siblings exhibit the mutant phenotype (23%, Fig 3.9 F).

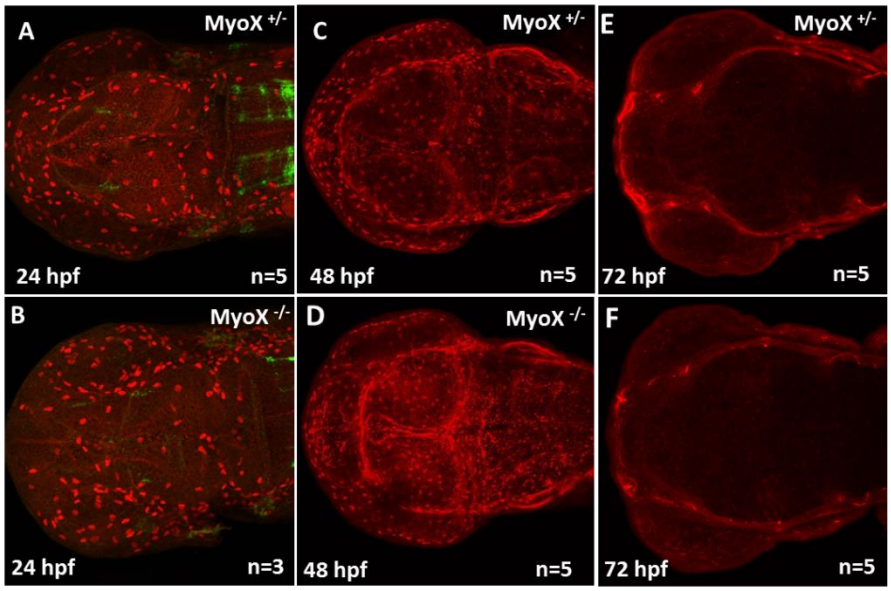

Fig 3.10 A-B) Wildtype (top) and *myoX* mutant (bottom) 24 hpf individuals, sox-10 stained showing neural crest cell migration. C-D) Wildtype (top) and MyoX mutant (bottom) 48 hpf individuals. E-F) Wildtype (top) and *myoX* mutant (bottom) 72 hpf individuals.

Wildtype NCC Counts Not Significantly Different From Mutant Siblings

Cranial neural crest cell migration was visualized using immunohistochemical staining. Anti sox-10 anti-bodies were used to stain cranial neural crest cells at different stages of development in both wildtype and mutant individuals from the same clutch. Once IHC staining was completed, cells were imaged using a Zeiss LSM 710 confocal microscope and

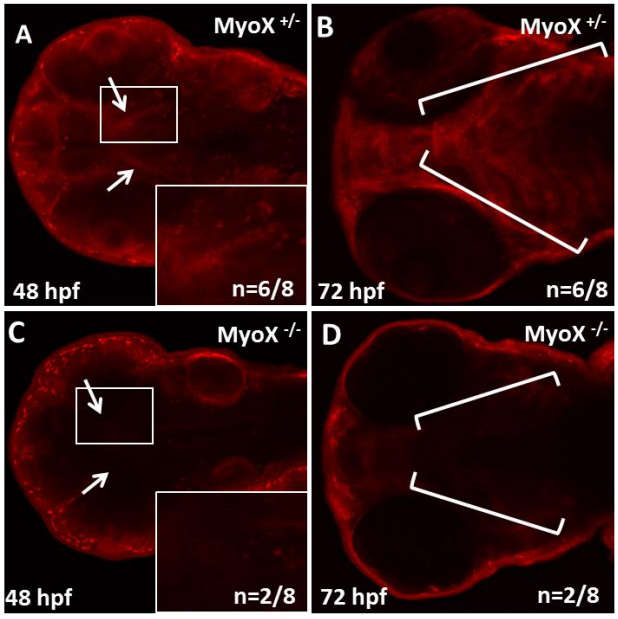

Fig 3.12 A-B) Wild type 48hpf and 72 hpf individuals, sox-10 stained showing neural crest cell migration. C-D) *MyoX* Mutant 48 hpf and 72 hpf individuals. Images shown are the bottom half of the embryos showing early craniofacial structure formation.

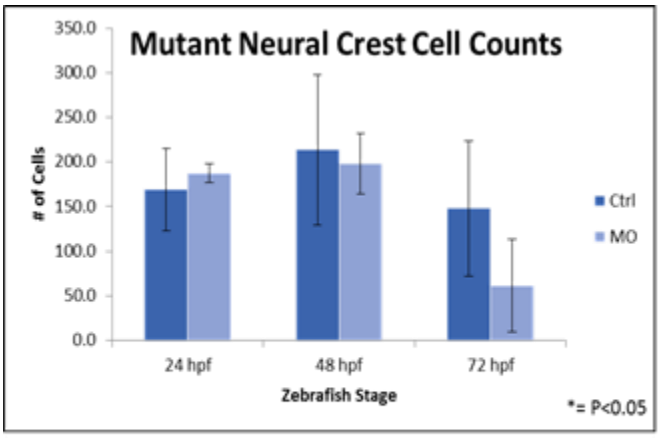

Fig 3.11Sox-10 stained individuals were counted using ImageJ image processing software. No groups were significantly different. P_{24h}= 0.53, P_{48h}= 0.74, P_{72h}=0.01. Bars indicate standard deviation.

processed using Zeiss Zen 2011 Black Edition software. 24 hpf wildtype and mutant individuals did not display any significant difference in cranial neural crest cell counts (P= 0.53, df=5, t= 2.57, $mean_{MUT}$=188.0 cells, $mean_{WT}$=169.3 cells, SD=46.0, 10.6) (Fig 3.10 A-B, Fig 3.11). 48 hpf wildtype and *myoX* mutant individuals also showed no significant difference in NCC counts (P= 0.74, df=7, t= 2.36, $mean_{MUT}$=198.3 cells, $mean_{WT}$=213.6 cells, SD=84.1, 34.1) (Fig 3.11 C-D, Fig 3.12). It follows that 72 hpf wildtype and *myoX* mutant individuals also displayed no significant difference in NCC counts (P= 0.1, df=8, t= 2.31, $mean_{MUT}$=64.1 cells, $mean_{WT}$=148.2 cells, SD=13.52, 31.64) (Fig 3.11 D-E, Fig 3.12).

Early Craniofacial Structures Absent in *MyoX* Mutant Individuals

Wildtype individuals begin to form craniofacial structures at 48hpf (Fig 3.12 A) while *myoX* mutant individual lack any organized craniofacial patterning at the same stage (Fig 3.12 C). These cell aggregations form the underlying patterns for craniofacial bone structures in zebrafish. By 72hpf, wildtype individuals show little to no NCC migratory cells (Fig 3.12 D) as craniofacial

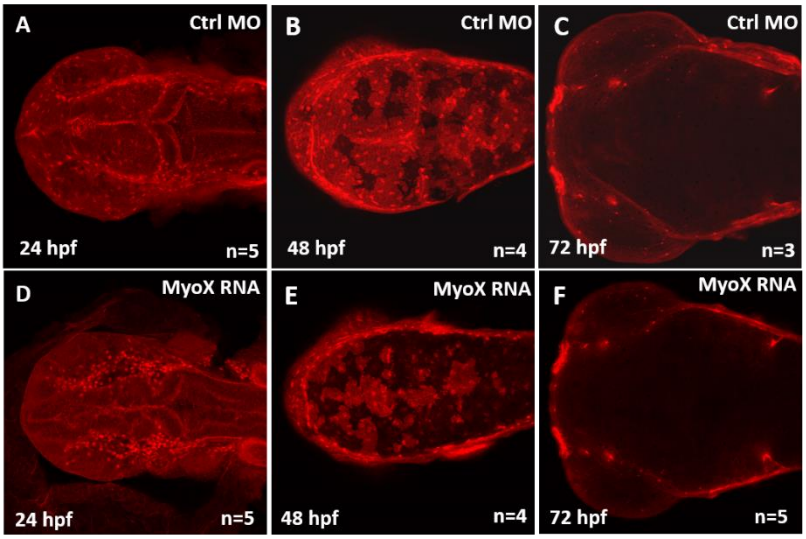

Fig 3.13 A/D) Control MO (top) and *myoX* muorphant (bottom) 24 hpf individuals, sox-10 stained showing neural crest cell migration. B/E) Control MO (top) and *myoX* morphant (bottom) 48 hpf individuals. C/F) Control MO (top) and *myoX* mophant (bottom) 72 hpf individuals.

structure patterning is heavily underway (Fig 3.12 B). Unlike the *myoX* morphant individuals, groups of cells are not present in *myoX* mutant individuals where these structures should be forming. This implies that NCC migratory pathways are much more obstructed in *myoX* mutant individuals than their morphant and wildtype counterparts.

Rescuability of Exogenous MyoX RNA

By reintroducing exogenous RNA into knockdown embryos, we hope to reverse *myoX* mutant and morphant phenotypes. This is also an effective method of accessing the effectiveness of the *myoX* knockdown, exogenous *myoX* RNA was co-injected into 2-8 cell stage wildtype zebrafish and phenotype was characterized in the same manner as previously described using mutant and morphant individuals. Prior to performing co-injections, over expression experiments were performed on 24, 48, and 72 hpf embryos (Fig 3.13. A-F). Morphological defects were documented in few (<5%) injected individuals at high concentrations of *myoX* RNA. NCC counts show no significant difference between uninjected control individuals and *myoX* RNA injected individuals at 24 and 72 hpf. However, 48 hpf *myoX* RNA injected individuals displayed significantly fewer NCC than the control individuals at the same developmental stage (Fig 3.14). When *myoX* RNA was co-injected with *myoX* MO, no significant change in NCC can be observed. Co-injected individuals at all observed stages (24, 48, and 72hpf) were statistically the same as *myoX* MO individuals. Control individuals were displayed significantly fewer NCC than both injected groups in 24 and 48 hpf individuals. No rescue of NCC migratory inhibition was observed in any of the observed developmental stages. Ventral craniofacial structures were not observed in rescue individuals (Fig 3.15-16).

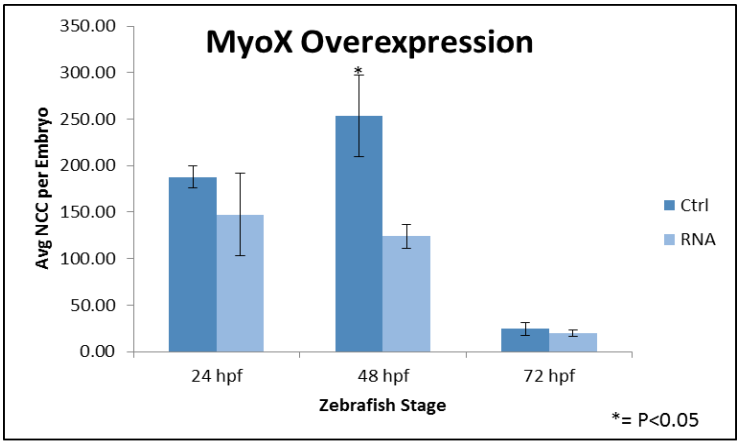

Fig 3.14 Sox-10 stained individuals were counted using ImageJ image processing software. Students T test analys was performed. Only 48 hpf groups were significantly different. P_{24h}= 0.2, P_{48h}< 0.01, P_{72h}=0.99. Bars indicate standard deviation.

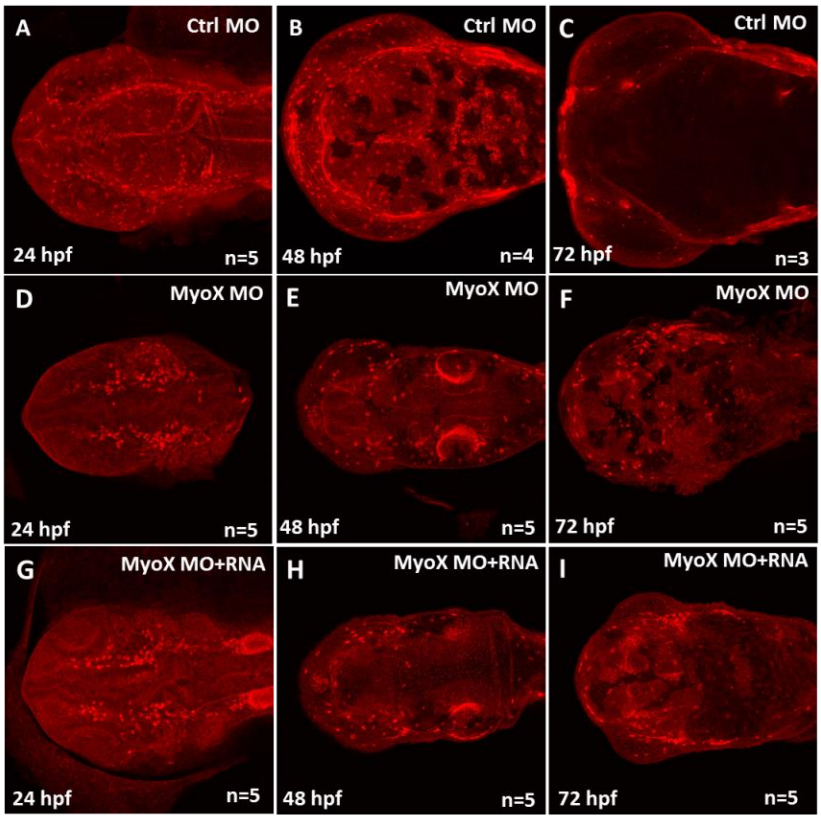

Fig 3.15 A,D,G) Control MO (top) and *myoX* muorphant (middle) and *myoX* MO+RNA (bottom) 24 hpf individuals, sox-10 stained showing neural crest cell migration. B,E, H) Control MO (top) and *myoX* morphant (middle) and *myoX* MO+RNA (bottom) 48 hpf individuals. C,F, I) Control MO (top) and *myoX* mophant (middle) and *myoX* MO+RNA (bottom) 72 hpf individuals.

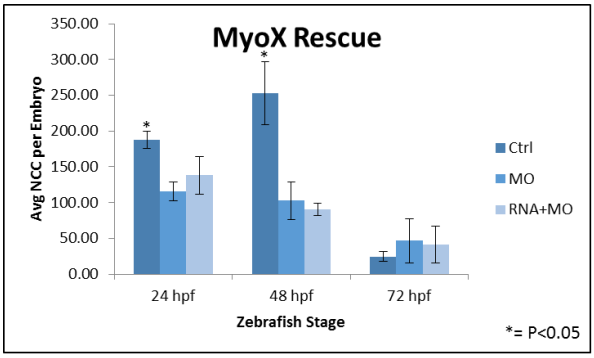

Fig 3.16 Sox-10 stained individuals were counted using ImageJ image processing software. Students T test analys was performed. Only 48 hpf groups were significantly different. P_{24h}= 0.2, P_{48h}< 0.01, P_{72h}=0.99. Bars indicate standard deviation.

CHAPTER 4

DISCUSSION

MyoX as a Downstream Responder to Intracellular Signaling Mechanisms

There are two major intracellular signaling pathways which regulate craniofacial development in zebrafish. The *Hedgehog* and *Wnt* signaling pathways transmit information to embryonic cells required for proper development (Cooper 2000). Different parts of the embryo have different concentrations of *Hedgehog* and *Wnt* signaling proteins in which cells respond to according to their cellular receptors (Ingham *et al.,* 2011). These signal transduction pathways are made of proteins that pass signals from outside of a cell through cell surface receptors to the inside of the cell. Both of these pathways end in activating transcription factors that are important for cranial neural crest cell specification and migration (Mohler, 1988). There have been several studies showing mutations within these signaling pathways lead to mutant craniofacial phenotypes similar to those seen in *myoX* mutant individuals.

Hedgehog (Hh) is a family of secreted glycoproteins that play a central role in the patterning of a variety of tissues and organs, including CNS, somites, limbs, bones, skin, lungs and testes (Hammerschmidt *et al.,* 1997; Murone *et al.,* 1999). Several membrane and intracellular proteins are important for transducing the *Hh* signal in the target cells. Genetic screens in *Drosophila* have identified *patched* (*ptc*), *smoothened* (*smo*), *fused* (*fu*), *cubitus interruptus* (*ci*) as crucial components of the Hh signaling machinery (Lin and Matsui 2012). It is thought that Hh binds to the transmembrane protein *Ptc*, that this causes dissociation of the *Ptc-Smo* complex at the membrane, and that the free *Smo* protein initiates intracellular signaling events including activation of Fused protein and conversion of *Ci* from a transcriptional repressor to an activator (Lin and Matsui 2012). Embryos containing mutations within the *smo* gene have expressed similar phenotypes to *myoX* morphant individuals.

Smo mutants have a ventrally curved body, small head with severe craniofacial defects and no outgrowth from the pectoral fin buds (Chen *et al.,* 2001). *Smo* mutant embryos at 120 hpf show smaller heads, posterior cyclopia, and absence of

cartilaginous jaw and brachial arches. In addition, a reduced cleithria and absence of pectoral fins (Chen *et al.,* 2001). This phenotype holds many of the same characteristics found in *myoX* morphant individuals. *MyoX* morphant individuals also displayed a shrunken head and a ventrally curved body. In addition, *myoX* morphants displayed an almost complete absence of cartilaginous jaw structures and branchial arches much like *smo* mutant phenotypes. This suggests a possible link between the *smoothened* protein and downstream molecules involved in craniofacial development such as *myoX.*

The *Wnt* gene family encodes a class of secreted signaling molecules involved in several neural crest processes in various organisms from *Drosophila* to vertebrates (LaBonne and Bronner-Fraser, 1998). Moreover, neural crest cell induction, facial patterning and morphogenesis are disrupted when *Wnt* signaling pathway is impaired, resulting in craniofacial malformations invertebrates (Brugmann *et al.,*2007) *Wnt* ligands function by binding to Frizzled receptors and activating downstream signaling including canonical *Wnt/β-catenin* and non-canonical *PCP* pathways (Lewis *et al.,* 2004; Tada *et al.,* 2002). Variations in *Wnt* signaling have been associated with both syndromic and non-syndromic cleft lip and palate anomalies (Juriloff *et al*., 2006). Previous studies have shown that the *Wnt*/*frizzled* signaling receptors *frzb* and *fzd7a* are necessary for chondrocyte proliferation, morphologic change and medio lateral intercalation to mediate palate extension. Further, *wnt9a*, *frzb* and *fzd7a* are necessary for lower jaw formation.

Frzb and *fzd7a* mophant individuals produced smaller craniofacial structures grossly and narrow mouth openings. The proximal trabeculae form and converge at the midline, but fail to elongate and the palate does not form (Kamel *et al.,* 2013). The chondrocytes in the leading edge of the trabeculae in *frzb* and *fzd7a* morphants appear dysmorphic and rounded and fail to adopt an organized intercalated pattern compared to wildtype individuals. In *frzb* and *fzd7a* morphants, the lower jaw is absent and undetected by Alcian blue cartilage staining (Kamel *et al.,* 2013). Similarly, *myoX* morphant individuals form portions of the trabeculae of the neurocranium which also converges at the midline yet fails to form the palate. The lower jaw of *myoX* mutants is also completely absent, much like the phenotype seen in *frzb* and *fzd7a* morphants.

This suggests a possible connection between upstream *wnt*/*frizzled* signaling pathways and downstream motor protein activity.

Many large scale craniofacial mutant screens have been performed in the past with several resulting phenotypes being similar in nature to the phenotype seen in this study (Neuhass *et al.* 1996; Schilling *et al.* 1996). For example, the *lockjaw (*allele ts213) mutation has a phenotype exhibiting a ventrally protruding jaw with restricted movements and reduced branchial arches. The *lockjaw* mutant phenotype is a result of a mutation in the *tfap2* gene, which is expressed in migrating neural crest cells (Knight *et al.,* 2003).The head and eyes remain slightly reduced and melanocytes are reduced throughout the body (Schilling *et al*. 1996). These results are similar to the phenotype seen in *myoX* mutant individuals which express a dwarfed head and eye regions along with a protruding jaw, indicating that *myoX* may have a similar role in craniofacial development.

By staining for migrating CNCCs, it is apparent that specification is not impaired in the mutant populations yet cells are not able to migrate and form the proper craniofacial structures during development (Kimmel *et al.,* 2002). CNCC specification occurs without any trouble yet is unable to form craniofacial structures due to migratory inhibition resulting from a truncated *myoX* motor protein. RNA in situ hybridization assays staining for *Tfap2* (Hoffman *et al., 2007)* and *Crestin* (Luo *et al., 2001)*, CNCC gene markers, indicate that CNCC cells are present in both wild type and mutant siblings but are unable to migrate to the craniofacial region properly in mutant individuals (Fig 3.9 A-B). The *myoX* mutation disrupts the expression of neural crest genes, much like what is seen using *myoX* MO in *Xenopus* (Nie *et al.,* 2009). It is possible that the transcription factor *tfap2* plays a key role in CNCC migration alongside *myoX.* I speculate that many other genes play critical roles in craniofacial development in conjuction with *myoX* however there is no known pathway established.

MyoX as a Responder to Extracellular Cues

In addition to intracellular signaling pathways, many genes expressed extracellularly must be present along with *myoX* for proper craniofacial development

(Spears and Svoboda 2005). *Fgf* signaling is inductive for neural crest formation (Monsoro-Burq *et al*, 2003, 2005), it also promotes the formation of chondrocyte lineage in the cranial neural crest (Monsoro-Burq et al, 2005). In advancing development, *Fgf* signaling is present in both the epithelia and mesenchyme and mediates the epithelial–mesenchymal interaction involved in almost all structure development. *Fgfr1* and *Fgfr2* are broadly expressed in the facial primordia (Bachler and Neubuser, 2001). Moreover, *Fgf*-dependent *Erk* activity has been reported in developing pharyngeal arches (Christen and Slack, 1999). In addition, it has recently been proposed that *Fgf* signals emanating from the neural tube might also influence neural crest development; specifically that *Fgf8* from the isthmus might repress *Hoxa2* expression in first arch crest, thereby specifying it to form first arch skeletal elements (Trainor et al., 2002).

Previous studies have shown that the inhibition of *Fgf* signaling results in the absence of all pharyngeal and neurocranial cartilages (Walsh and Mason 2003). Using morpholino oligonucleotides to inhibit individual members of the family, it was shown that *Fgf3* is required for the formation of all cartilage elements derived from pharyngeal arches 1-4. While inhibition of *Fgf8* by itself had little to no effect on cartilage formation, inhibition of both *Fgf3* and *Fgf8* together resulted in an almost complete absence of cranial and pharyngeal cartilages (Walsh and Mason 2003). When using lower concentrations of the *Fgf3mo*, all cartilage derivatives of the first and second arches were present and identifiable but somewhat dysmorphic. Most notably, the ceratohyal elements projected posteriorly rather than anteriorly; however, this did not represent a reversal in second arch polarity as the midline basihyal elements still projected anteriorly (Walsh and Mason 2003). The fifth ceratobranchial cartilage, easily identifiable by its pharyngeal teeth, was present and apparently normal. However, the ceratobranchial elements derived from arches 1-4 were greatly reduced in size when compared with embryos injected with the control morpholino (Walsh and Mason 2003).

The *Fgf3/8mo* phenotypes are comparable to the *myoX* mutant phenotype found in this study. Much like the *Fgfmo* phenotypes, *myoX* mutant individuals displayed developmental defects in both the ceratohyal and ceratobranchial arches. The angle formed in *myoX* mutant individuals was nearly twice as obtuse as those found in control individuals, much like the *Fgfmo* individuals. Ceratobrachial arches 1-4 are largely

missing in *myoX* mutant individuals however the tooth bearing fifth ceratobranchial arch is largely unaffected, much like *Fgfmo* individuals. Given the similarities in mutant phenotypes, I speculate that these genes are working together in similar signaling pathways necessary for fibroblast projections and ultimately cellular migration. *Fgf* is involved in extracellular signaling, possibly upstream of *myoX* activity. It is possible that both studies are showing the same signaling pathway being disrupted at different points, thus giving similar phenotypes.

Additionally, it has been shown that extracellular retinoic acid (RA) signaling influences endodermal pouch development at different embryonic stages. It is understood that RA affects pharyngeal arch development because of the phenotypes observed in infants whose mothers were exposed to high levels of Vitamin A during pregnancy (de Die-Smulders et al., 1995). In addition, these defects can be phenocopied by treating pregnant experimental animals with vitamin A (a precursor of RA) or synthetic RA (Davis and Sadler, 1981; Scambler, 2000). Also, genetic disruption of the RA signaling pathway leads to defects in structures derived from pharyngeal arches 3–4 in mice and zebrafish (Matt et al., 2003; Niederreither et al., 2003). While extensive evidence exists implicating RA signaling in pharyngeal arch development, it is not as clear on which cells or tissues of the developing arches RA may act upon.

In embryos treated with diethylaminobenzaldehyde (DEAB), a potent inhibitor of the enzyme retinaldehyde dehydrogenase (RALDH) that converts retinal to RA during gastrulation, the cartilages of the mandibular and hyoid arches are present but smaller in size and misshapen (Kopinke *et al,* 2006). Cartilages of the posterior arches (2-5) are absent. Even though neural crest cells are present in the posterior pharyngeal arches of embryos treated with DEAB post-gastrulation, they do not differentiate into cartilage. Cartilages derived from neural crest cells of the first and second pharyngeal arches are reduced but present in RA-depleted embryos, while cartilages of pharyngeal arch 3 are reduced and cartilages of arches 4–5 are absent (Rhinn and Dolle 2012).

Much like the previous example, the *myoX* mutant phenotype resembles that which was found in the DEAB treated individuals, specifically in the ceratobranchial arches. I found a reduction in the number of cells in mutant individuals as well as misshapen structures, much like those individuals treated with DEAB. A majority of the

posterior cartilage structures were absent in *myoX* mutant individuals. This pattern can also be found in RA inhibited individuals. By comparing the similarities between DEAB treated and *myoX* mutant individuals, I am suggesting that RA signaling may be upstream of MyoX and similar motor proteins responsible for filopodial protrusions and cell migration during development.

MyoX in Filopodial Extensions

I have shown that there is a possible connection between both intracellular and extracellular signaling pathways, *myoX,* and craniofacial development. These signaling pathways are in place to activate *myoX* at the tips of filopodial extensions (Tokuo *et al.*, 2007). *MyoX* is a major actin binding protein that activates and regulates filopodial dynamics necessary for cell migration (Zhu *et al.,* 2007). Recent studies have revealed that *myoX* has an important role in the elongation of filopodia (Berg and Cheney, 2002). The N-terminal domain of *myoX* functions as a motor domain, which is followed by a neck region. The predicted coiled-coil segment is present at the C-terminal side of the neck region (Berg *et al*., 2000). The C-terminal end of the molecule is the tail domain that was reported as a binding portion to the specific cargo molecules (Tokuo and Ikebe, 2004). Because *myoX* moves toward the tip of filopodia and transports the cargo molecules, the function of *myoX* was thought to simply be that of a cargo carrier. However, studies have shown that the motor activity of *myoX* is itself critical for the initiation of filopodia formation (Tokuo *et al.*, 2007).

Similar studies have been performed demonstrating that *myoX* is selectively expressed in premigratory and migrating neural crest cells in the early *Xenopus* embryo and that it plays a critical role in their migration, partly by influencing cell adhesive interactions (Nie and Bronner-Fraser 2009). Based on the craniofacial cartilage characterization results seen in Chapter 3, it is likely that the disruption of proper MyoX protein formation is inhibiting the filopodial-tip complex from forming. Without this formation, cell migration is virtually impossible within the embryo. Although little is known about the role of MyoX in filopodial formation, one can speculate based on

previous work that without MyoX these filopodial protrusions will not form, thus inhibiting cellular migration through the developing embryo.

MyoX has several distinguished cellular features as compared with other unconventional myosin family proteins. It is primarily localized at the tips of filopodia or the edges of lamellipodia and membrane ruffles (Berg and Cheney, 2002). It undergoes forward and rearward movements within filopodia and promotes filopodia formation, elongation and sensing, possibly by transporting actin-binding proteins and cell adhesion receptors to the leading edge of the cell (Tokuo and Ikebe, 2004). It is widely expressed and implicated in multiple cellular functions in different cell types, including netrin-1-induced neurite outgrowth and growth-cone guidance (Zhu *et al.*, 2007), *BMP6*-dependent filopodial migration and activation of *BMP* receptors (Pi *et al.*, 2007), and migration of *Xenopus* cranial neural crest cells (Hwang *et al.*, 2009; Nie *et al.*, 2009).

MyoX has been show to regulate netrin receptors and functions in axonal path-finding during neural development (Zhu *et al.,* 2007). It has been shown to play an important role in filopodium formation by transportation of specific cargos within the cell (Liu *et al., 2012).* The nonsense mutation induced within our zebrafish model creates a premature stop codon which lies somewhere within the coil-coiled dimer structure of the MyoX motor protein. By truncating this region of the protein, we speculate that the FERM domains of the protein are not able to form properly, thus inhibiting any domain interactions between MyoX and its cargo/extracellular integrins.

During cell migration, the protrusive leading edge plays a key role in directional movement (Ridley *et al.*, 2003). The leading edge of the migrating cells consists of the two types of actin cytoskeletal architectures, lamellipodia and filopodia. Filopodia is the structure protruding from the edge of the cells that plays an essential role in the wide range of cell motile activities, including cancer cell migration (Wicki *et al.,* 2006) and neuronal path finding (Bentley and O'Connor, 1994). Although many studies have been conducted on the role of actin-binding proteins in the actin dynamics at membrane protrusion (Nakagawa *et al.*, 2003; Biyasheva *et al.*, 2004), little is known about the role of the actin-based motor protein myosin in filopodia formation. However, I speculate that *myoX* inhibition is keeping these filopodial extensions from forming, which is turn inhibits

forward cellular movement. More studies need to be conducted to investigate the nature of this complex.

Future Directions

To further investigate the effects of *myoX* knockdown, a *sox-10* transgenic line of zebrafish can be obtained and used to live image migrating cells. By observing embryos at specific larval stages, we are simply taking a snapshot at very complex and dynamic processes. Real time NCC migration imaging would allow us to see the entire process, not just moments in time. *MyoX* is thought to be localized at filopodial tips (Mattila and Lappalainen, 2008), so live imagining would allow us to visualize these cellular extensions. By comparing cellular movements between treatment and control groups, cellular projections and CNCC migration can be linked with the MyoX motor protein (Kwak *et al., 2013).*

Across all three stage groups of *myoX* morphant individuals, the number of CNCC remained relatively constant, indicating that the lack of structures in these individuals isn't due to premature cellular apoptosis, rather the inability to migrate into their proper cartilage structure locations. These findings coincide with previous work done in *xenopus* that CNCC migration and stream formation are abnormal after *myoX* knockdown events (Nie *et al*., 2009). To ensure that the cells are not migrating due to inhibition of *myoX*, specific cell death can be visualized through anti body staining. This will prove that the NCCs are specifying and staying alive but not migrating to their final location for differentiation, which is essential for proper craniofacial development.

Because CNCCs acquire much of their differentiation potential by inductive interactions during and after migration (Le Douarin *et al.*, 2004), it is possible that *myoX* knockdown CNCCs are unable to receive such inductive cues, leading to a failure to differentiate properly. To conclusively say that the craniofacial structure deformities are a result of cellular migration inhibition and not the inability to differentiate, the transgenic line *Fli*I*/GFP* can be implemented into this study. This line of transgenic zebrafish will allow us to visualize craniofacial chondrocyte differentiation.

MO specificity can be addressed in a variety of ways. One commonly used approach for phenotypes observed in the first 24–48 h of development is to reverse the

noted effects by a strategy called RNA “rescue” (Bill *et al, 2009)*. *MyoX* rescue experiments were performed on *myoX* MO individuals and compared to control individuals to assess the effectiveness of the *myoX* morpholino. However, the phenotype was not rescued in any *myoX* MO+RNA individuals. There are many reasons to possibly explain this. This particular protein may be very time sensitive in its effectiveness to NCC migration, and missing that specific time frame by only a few hours may prevent the injected RNA from rescuing the phenotype. Furthermore, a MYC tag (a polypeptide protein tag derived from the c-myc gene product that can be added to a protein using recombinant DNA technology) was inserted into the RNA construct to allow easy identification of the expressed protein. MYC tag anti body staining was performed on rescue individuals but results were inconclusive to the presence of this tag. This staining will allow us to easily visualize if the exogenous RNA is being expressed as a protein.

The cartilage structure phenotype seen in other mutants is very similar in *myoX* mutants but melanocyte quantification in *myoX* mutants has not been performed. CNCCs also differentiate into melanocytes which suggest that CNCCs are involved in this particular mutation as well. A valuable way of characterizing the *myoX* phenotype would be to quantify the melanocytes in developing zebraifsh (Schilling *et al.* 1996). This will generate data with regards to CNCC migration in *myoX* mutants.

In conclusion, this study has shown that in both morphant and mutant individuals, *myoX* is required for craniofacial development in zebrafish. *MyoX* morphant individuals display near total loss of craniofacial cartilage structures while maintaining CNCC integrity as seen in their IHC staining assays. Different stages of morphant individuals maintain the same relative number of cells indicating problems within the migratory pathways of these cells and that the loss of structures is not due to premature cell death but as a result of inhibited migration. Mutant individuals exhibited similar loss of craniofacial structures while maintaining cellular shape and size. These findings remain constant with previous studies involving *in vitro* cultures and cell dissociation–reaggregation assays which suggested that *myoX* may be required for cell protrusion and cell–cell adhesion (Nie *et al*., 2009; Hwang *et al.,* 2009).

REFERENCES

ABERCROMBIE, M., & HEAYSMAN, J. E. (1953). Observations on the social behavior of cells in tissue culture. I. speed of movement of chick heart fibroblasts in relation to their mutual contacts. Experimental Cell Research, 5(1), 111-131. Retrieved from https://search-ebscohost-com.libez.lib.georgiasouthern.edu/login.aspx?direct=true&db=cmedm&AN=13083622&site=eds-live

Alberts, B., Johnson, A., & Lewis, J. (2002). Molecular biology of the cell. 4th edition.. Garland Science,

Bachler M, Neubuser A (2001). Expression of members of the Fgf family and their receptors during midfacial development. Mech Dev 100: 313–316.

Barth, K. A., Kishimoto, Y., Rohr, K. B., Seydler, C., Schulte-Merker, S., & Wilson, S. W. (1999). Bmp activity establishes a gradient of positional information throughout the entire neural plate. Development (Cambridge, England), 126(22), 4977-4987. Retrieved from https://search-ebscohost-com.libez.lib.georgiasouthern.edu/login.aspx?direct=true&db=cmedm&AN=10529416&site=eds-live

Bentley, D., & O'Connor, ,T.P. (1994). Cytoskeletal events in growth cone steering. Current Opinion in Neurobiology, 4(1), 43-48. Retrieved from https://search.ebscohost.com/login.aspx?direct=true&db=mnh&AN=8173324&site=eds-live

Berg, J. S., & Cheney, R. E. (2002). Myosin-X is an unconventional myosin that undergoes intrafilopodial motility. Nature Cell Biology, 4(3), 246. Retrieved from https://search-ebscohost-com.libez.lib.georgiasouthern.edu/login.aspx?direct=true&db=ofm&AN=8783700&site=eds-live

Berg, J.S. et al. (2000) Myosin-X, a novel myosin with pleckstrin homology domains, associates with regions of dynamic actin. J. Cell Sci. 113, 3439–3451

Bill, B. R., Petzold, A. M., Clark, K. J., Schimmenti, L. A., & Ekker, S. C. (2009). A primer for morpholino use in zebrafish. Zebrafish, (1), 69. Retrieved from https://search-ebscohost-com.libez.lib.georgiasouthern.edu/login.aspx?direct=true&db=edsgao&AN=edsgcl.200117995&site=eds-live

Biyasheva, A., Svitkina, T., Kunda, P., Baum, B., & Borisy, G. (2004). Cascade pathway of filopodia formation downstream of SCAR. Journal of Cell Science, 117, 837-848. Retrieved from

https://search.ebscohost.com/login.aspx?direct=true&db=mnh&AN=14762109&site=eds-live

Bridgman, P.C. et al. (2001) Myosin IIB is required for growth cone motility. J. Neurosci. 21, 6159–6169

Bron, R., Eickholt, B. J., Vermeren, M., Fragale, N., & Cohen, J. (2004). Functional knockdown of neuropilin-1 in the developing chick nervous system by siRNA hairpins phenocopies genetic ablation in the mouse. Developmental Dynamics: An Official Publication of the American Association of Anatomists, 230(2), 299-308. Retrieved from https://search-ebscohost-com.libez.lib.georgiasouthern.edu/login.aspx?direct=true&db=cmedm&AN=15162508&site=eds-live

Bronner, M. (2012). Formation and migration of neural crest cells in the vertebrate embryo. Histochemistry & Cell Biology, 138(2), 179. doi:10.1007/s00418-012-0999-z

Bruder, S. P., & Caplan, A. I. (1989). First bone formation and the dissection of an osteogenic lineage in the embryonic chick tibia is revealed by monoclonal antibodies against osteoblasts. Bone, 10(5), 359-375. Retrieved from https://search-ebscohost-com.libez.lib.georgiasouthern.edu/login.aspx?direct=true&db=cmedm&AN=2481484&site=eds-live

Brugmann, S.A., Goodnough, L.H., Gregorieff, A., Leucht, P., ten Berge, D., Fuerer, C., Clevers, H., Nusse, R., Helms, J.A., 2007. Wnt signaling mediates regional specification in the vertebrate face. Development 134, 3283–3295.

Burns, A. J., & Douarin, N. M. (1998). The sacral neural crest contributes neurons and glia to the post-umbilical gut: Spatiotemporal analysis of the development of the enteric nervous system. Development (Cambridge, England), 125(21), 4335-4347. Retrieved from https://search.ebscohost.com/login.aspx?direct=true&db=mnh&AN=9753687&site=eds-live

Carney, T. J., Dutton, K. A., Greenhill, E., Delfino-Machín, M., Dufourcq, P., Blader, P., et al. (2006). A direct role for Sox10 in specification of neural crest-derived sensory neurons. Development (Cambridge, England), 133(23), 4619-4630. Retrieved from https://search-ebscohost-com.libez.lib.georgiasouthern.edu/login.aspx?direct=true&db=cmedm&AN=17065232&site=eds-live

Chang, C., & Hemmati-Brivanlou, A. (1998). Neural crest induction by Xwnt7B in xenopus. Developmental Biology, 194(1), 129-134. Retrieved from https://search-ebscohost-

com.libez.lib.georgiasouthern.edu/login.aspx?direct=true&db=cmedm&AN=9473337&site=eds-live

Chen, W., Burgess, S., & Hopkins, N., (2001). Analysis of the zebrafish smoothened mutant reveals conserved and divergent functions of hedgehog activity. Development 128, 2385-2396.

Christen, B., Slack, J.M., (1999) Spatial response to fibroblast growth factor signalling in Xenopus embryos. Development 126, 119–125.

Coles, E. G., Gammill, L. S., Miner, J. H., & Bronner-Fraser, M. (2006). Abnormalities in neural crest cell migration in laminin α5 mutant mice. Developmental Biology, 289, 218-228. doi:10.1016/j.ydbio.2005.10.031 A direct role for Sox10 in specification of neural crest-derived sensory neurons Retrieved from https://search.ebscohost.com/login.aspx?direct=true&db=edsoai&AN=edsoai.784255800&site=eds-live; http://hal.archives-ouvertes.fr/hal-00169710

Cordero, D. R., Brugmann, S., Chu, Y., Bajpai, R., Jame, M., & Helms, J. A. (2011). Cranial neural crest cells on the move: Their roles in craniofacial development. American Journal of Medical Genetics.Part A, 155A(2), 270-279. doi:10.1002/ajmg.a.33702

Cserjesi, P., Brown, D., Ligon, K. L., Lyons, G. E., Copeland, N. G., Gilbert, D. J., et al. (1995). Scleraxis: A basic helix-loop-helix protein that prefigures skeletal formation during mouse embryogenesis. Development (Cambridge, England), 121(4), 1099-1110. Retrieved from https://search-ebscohost-com.libez.lib.georgiasouthern.edu/login.aspx?direct=true&db=cmedm&AN=7743923&site=eds-live

Davis LA, Sadler TW. (1981) Effects of vitamin A on endocardial cushion development in the mouse heart. Teratology 24: 139–148.

de Die-Smulders CE, Sturkenboom MC, Veraart J, van Katwijk C, Sastrowijoto P, van der Linden E. (1995) Severe limb defects and craniofacial anomalies in a fetus conceived during acitretin therapy. Teratology 52:215–219.

Donoghue, P. C. J., Graham, A., & Kelsh, R. N. (2008). The origin and evolution of the neural crest. Bioessays: News and Reviews in Molecular, Cellular and Developmental Biology, 30(6), 530-541. doi:10.1002/bies.20767

Draper, B. W., Morcos, P. A., & Kimmel, C. B. (2001). Inhibition of zebrafish fgf8 pre-mRNA splicing with morpholino oligos: A quantifiable method for gene knockdown. Genesis (New York, N.Y.: 2000), 30(3), 154-156. Retrieved from https://search-ebscohost-

com.libez.lib.georgiasouthern.edu/login.aspx?direct=true&db=cmedm&AN=11477696&site=eds-live

Farlie, P. G., Kerr, R., Thomas, P., Symes, T., Minichiello, J., Hearn, C. J., et al. (1999). A paraxial exclusion zone creates patterned cranial neural crest cell outgrowth adjacent to rhombomeres 3 and 5. Developmental Biology, 213(1), 70-84. Retrieved from https://search-ebscohost-com.libez.lib.georgiasouthern.edu/login.aspx?direct=true&db=cmedm&AN=10452847&site=eds-live

Fayez, F., Safadi, M. F., Barbe, S. M., Abdelmagid, M. C., Rico, R. A., Aswad, J., et al. (2009). Bone structure, development and bone biology . Bone Pathology,

Gilbert, S. F. (2000). Developmental biology. Developmental Biology., 6th edition, http://www.ncbi.nlm.nih.gov/books/NBK10065/.

Gorlin, R. J., Cohen, M. M., & Levin, L. S. (1990). Syndromes of the head and neck / robert J. gorlin, M. michael cohen, jr., L. stefan levin New York : Oxford University Press, 1990; 3rd ed. Retrieved from https://search-ebscohost-com.libez.lib.georgiasouthern.edu/login.aspx?direct=true&db=edshlc&AN=edshlc.002138854-7&site=eds-live

Hadeball, B., Borchers, A., & Wedlich, D. (1998). Xenopus cadherin-11 (xcadherin-11) expression requires the Wg/Wnt signal. Mechanisms of Development, 72(1–2), 101-113. doi:http://dx.doi.org.libez.lib.georgiasouthern.edu/10.1016/S0925-4773(98)00022-7

Hall, B. K. (2009). The neural crest and neural crest cells in vertebrate development and evolution. New York, NY: Springer. Retrieved from https://search-ebscohost-com.libez.lib.georgiasouthern.edu/login.aspx?direct=true&db=edsebk&AN=275664&site=eds-live

Hall, B. K., & Gillis, J. A. (2013). Incremental evolution of the neural crest, neural crest cells and neural crest-derived skeletal tissues. Journal of Anatomy, 222(1), 19-31. doi:10.1111/j.1469-7580.2012.01495.x

Hammerschmidt, M., Brook, A. and McMahon, A. P. (1997). The world according to hedgehog. Trends Genet. 13, 14-21.

Hanken, J., & Gross, J. B. (2005). Evolution of cranial development and the role of neural crest: Insights from amphibians. Journal of Anatomy, 207(5), 437-446. doi:10.1111/j.1469-7580.2005.00481.x

Hanken, J., & Hall, B. K. (1988). Skull development during anuran metamorphosis. II. role of thyroid hormone in osteogenesis. Anatomy and Embryology, 178(3), 219-227. Retrieved from

https://search.ebscohost.com/login.aspx?direct=true&db=mnh&AN=3414976&site=eds-live

Hanna, L. A., Foreman, R. K., Tarasenko, I. A., Kessler, D. S., & Labosky, P. A. (2002). Requirement for Foxd3 in maintaining pluripotent cells of the early mouse embryo. Genes & Development, (20), 1650. Retrieved from https://search-ebscohost-com.libez.lib.georgiasouthern.edu/login.aspx?direct=true&db=edsgao&AN=edsgcl.95793251&site=eds-live

Hoffman T., Javier A., Campeau S., Knight R., Schilling T., (2007) Tfap2 transcription factors in zebrafish neural crest development and ectodermal evolution. J Exp Zool B Mol Dev Evol. 2007 Sep 15; 308(5): 679-91. PMID: 17724731

Horton, W. A. (1990). The biology of bone growth. Growth Genet. Horm., 6(1-3) Hyatt, T. M., & Ekker, S. C. (1999). Vectors and techniques for ectopic gene expression in zebrafish. Methods in Cell Biology, 59, 117-126. Retrieved from https://search-ebscohost-com.libez.lib.georgiasouthern.edu/login.aspx?direct=true&db=cmedm&AN=9891358&site=eds-live

Hwang, Y., Luo, T., Xu, Y., & Sargent, T. D. (2009). Myosin-X is required for cranial neural crest cell migration in xenopus laevis. Developmental Dynamics: An Official Publication of the American Association of Anatomists, 238(10), 2522-2529. doi:10.1002/dvdy.22077

Ingham, Philip W.; Nakano, Yoshiro; Seger, Claudia (2011). Mechanisms and functions of Hedgehog signalling across the metazoa. Nature Reviews Genetics 12 (6): 393–406. doi:10.1038/nrg2984. PMID 21502959

Jackman, W. R., Draper, B. W., & Stock, D. W. (2004). Fgf signaling is required for zebrafish tooth development. Developmental Biology, 274(1), 139-157. doi:http://dx.doi.org.libez.lib.georgiasouthern.edu/10.1016/j.ydbio.2004.07.003

Javidan, Y., & Schilling, T. F. (2004). Development of cartilage and bone. Methods in Cell Biology, 76, 415-436. Retrieved from https://search-ebscohost-com.libez.lib.georgiasouthern.edu/login.aspx?direct=true&db=cmedm&AN=15602885&site=eds-live

Juriloff, D.M.,Harris,M.J.,McMahon,A.P.,Carroll,T.J.,Lidral,A.C.,2006.Wnt9b is the mutated gene involved in multifactorial non syndromic cleft lip with or without cleft palatein A/Wy Sn mice, as confirmed by a genetic complementation test. Birth DefectsRes.AClin.Mol.Teratol.76, 574–579.

Kamel, G., Hoyos, T., Rochard, L., Dougherty, M., Kong, Y., Tse, W., Shubinets, V., Grimaldi, M., Liao, E., (2013). Requirement for frzb and fzd7a in cranial neural

crest convergence and extension mechanisms during zebrafish palate and jaw morphogenesis. Developmental Biology 381 (2013) 423–433. http://dx.doi.org/10.1016/j.ydbio.2013.06.012

Kasemeier-Kulesa, J., Kulesa, P. M., & Lefcort, F. (2005). Imaging neural crest cell dynamics during formation of dorsal root ganglia and sympathetic ganglia. Development (09501991), 132(2), 235-245. doi:10.1242/dev.01553

Kasemeier-Kulesa, J., Teddy, J. M., Postovit, L., Seftor, E. A., Seftor, R. E. B., Hendrix, M. J. C., et al. (2008). Reprogramming multipotent tumor cells with the embryonic neural crest microenvironment. Developmental Dynamics: An Official Publication of the American Association of Anatomists, 237(10), 2657-2666. doi:10.1002/dvdy.21613

Kettleborough, R., Busch-Nentwich, E., Harvey, S. A., Dooley, C. M., de Bruijn, E., van Eeden, F., et al. (2013). A systematic genome-wide analysis of zebrafish protein-coding gene function Retrieved from https://search-ebscohost-com.libez.lib.georgiasouthern.edu/login.aspx?direct=true&db=edswsc&AN=000317984400039&site=eds-live

Kimmel, C. B., Ballard, W. W., Kimmel, S. R., Ullmann, B., & Schilling, T. F. (1995). Stages of embryonic development of the zebrafish. Developmental Dynamics: An Official Publication of the American Association of Anatomists, 203(3), 253-310. Retrieved from https://search-ebscohost-com.libez.lib.georgiasouthern.edu/login.aspx?direct=true&db=cmedm&AN=8589427&site=eds-live

Kimmel, C. B., Miller, C. T., & Moens, C. B. (2001). Review article: Specification and morphogenesis of the zebrafish larval head skeleton. Developmental Biology, 233, 239-257. doi:10.1006/dbio.2001.0201

Kimmel, C. B., Miller, C. T., & Moens, C. B. (2001). Review article: Specification and morphogenesis of the zebrafish larval head skeleton. Developmental Biology, 233, 239-257. doi:10.1006/dbio.2001.0201

Kirby, M. L. (1987). Cardiac morphogenesis--recent research advances. Pediatric Research, 21(3), 219-224. Retrieved from https://search-ebscohost-com.libez.lib.georgiasouthern.edu/login.aspx?direct=true&db=cmedm&AN=3562119&site=eds-live

Kirby, M. L., & Waldo, K. L. (1990). Role of neural crest in congenital heart disease. Circulation, 82(2), 332-340. Retrieved from https://search-ebscohost-com.libez.lib.georgiasouthern.edu/login.aspx?direct=true&db=cmedm&AN=2197017&site=eds-live

Klymkowsky, M. W., Rossi, C. C., & Artinger, K. B. (2010). Mechanisms driving neural crest induction and migration in the zebrafish and xenopus laevis. Cell Adhesion

& Migration, 4(4), 595-608. Retrieved from https://search.ebscohost.com/login.aspx?direct=true&db=mnh&AN=20962584&site=eds-live

Knight, R. D., & Schilling, T. F. (2006). Cranial neural crest and development of the head skeleton. Advances in Experimental Medicine and Biology, 589, 120-133. Retrieved from https://search.ebscohost.com/login.aspx?direct=true&db=mnh&AN=17076278&site=eds-live

Kight R., Nair S., Nelson S., Afshar A., Javidan Y., Geisler R., Rauch G-J. and Schilling T., (2003). Lockjaw encodes a zebrafish tfap2a required for early neural crest development. Development 130, 5755-5768. doi:10.1242/dev.00575

Kopinke, D., Sasine, J., Swift, J., Stephens, W. Z., & Piotrowski, T. (2006). Retinoic Acid Is Required for Endodermal Pouch Morphogenesis and Not for Pharyngeal Endoderm Specification. Developmental Dynamics 235:2695–2709, 2006. DOI 10.1002/dvdy.20905

Kulesa, P. M., & Fraser, S. E. (1998). Neural crest cell dynamics revealed by time-lapse video microscopy of whole embryo chick explant cultures. Developmental Biology, 204(2), 327-344. doi:http://dx.doi.org.libez.lib.georgiasouthern.edu/10.1006/dbio.1998.9082

Kulesa, P. M., Bailey, C. M., Kasemeier-Kulesa, J., & McLennan, R. (2010). Cranial neural crest migration: New rules for an old road. Developmental Biology, (2), 543. doi:10.1016/j.ydbio.2010.04.010

Kwak, J., Park, O., Jung, Y., Hwang, B., Kwon, S., & Kee, Y. (2013). Live image profiling of neural crest lineages in zebrafish transgenic lines. Molecules & Cells, 35(3), 255-260. doi:10.1007/s10059-013-0001-5

LaBonne, C.,Bronner-Fraser,M.,1998.Neural crest induction in Xenopus: evidence for a two-signal model. Development125,2403–2414.

Langford, G. M. (1995). Actin- and microtubule-dependent organelle motors: Interrelationships between the two motility systems. Current Opinion in Cell Biology, 7(1), 82-88. Retrieved from https://search-ebscohost-com.libez.lib.georgiasouthern.edu/login.aspx?direct=true&db=cmedm&AN=7755993&site=eds-live

Lawrence, C. (2007). The husbandry of zebrafish (danio rerio): A review. Aquaculture, 269(1–4), 1-20. doi:http://dx.doi.org.libez.lib.georgiasouthern.edu/10.1016/j.aquaculture.2007.04.077

Le Douarin, ,N.M., & Teillet, M. A. (1973). The migration of neural crest cells to the wall of the digestive tract in avian embryo. Journal of Embryology and Experimental Morphology, 30(1), 31-48. Retrieved from https://search-ebscohost-com.libez.lib.georgiasouthern.edu/login.aspx?direct=true&db=cmedm&AN=4729950&site=eds-live

Le Douarin, N. (1982). The neural crest / nicole le douarin Cambridge Cambridgeshire] ; New York : Cambridge University Press, 1982. Retrieved from https://search-ebscohost-com.libez.lib.georgiasouthern.edu/login.aspx?direct=true&db=edshlc&AN=edshlc.000590314-9&site=eds-live

Le Douarin, N. M., Creuzet, S., Couly, G., & Dupin, E. (2004). Neural crest cell plasticity and its limits. Development (09501991), 131(19), 4637-4650. doi:10.1242/dev.01350

Le Douarin, N., & Kalcheim, C. (1999). The neural crest / nicole M. le douarin and chaya kalcheim Cambridge, U.K. ; New York, NY, USA : Cambridge University Press, 1999; 2nd ed. Retrieved from https://search-ebscohost-com.libez.lib.georgiasouthern.edu/login.aspx?direct=true&db=edshlc&AN=edshlc.008556759-0&site=eds-live

Le Lièvre, C. S., & Le Douarin, ,N.M. (1975). Mesenchymal derivatives of the neural crest: Analysis of chimaeric quail and chick embryos. J. Embryol. Exp. Morph., 34(1), 125-154.

LeClair, E. E., Mui, S. R., Huang, A., Topczewska, J. M., & Topczewski, J. (2009). Craniofacial skeletal defects of adult zebrafish glypican 4 (knypek) mutants. Developmental Dynamics: An Official Publication of the American Association of Anatomists, 238(10), 2550-2563. doi:10.1002/dvdy.22086

Lewis, J.L., Bonner, J., Modrell, M., Ragland, J.W., Moon, R.T., Dorsky, R.I., Raible, D.W., 2004. Reiterated Wnt signaling during zebra fish neural crest development. Development131, 1299–1308.

Li, M., Zhao, C., Wang, Y., Zhao, Z., & Meng, A. (2002). Zebrafish sox9b is an early neural crest marker. Development Genes and Evolution, 212(4), 203-206. Retrieved from https://search-ebscohost-com.libez.lib.georgiasouthern.edu/login.aspx?direct=true&db=mnh&AN=12012235&site=eds-live

Lin, T., & Matsui, W., (2012). Hedgehog pathway as a drug target: Smoothened inhibitors in development. OncoTargets and Therapy 2012:5 47–58. http://dx.doi.org/10.2147/OTT.S21957

Liu, Y., & Semina, E. V. (2012). pitx2 deficiency results in abnormal ocular and craniofacial development in zebrafish. Plos One, 7(1), 1-9. doi:10.1371/journal.pone.0030896

Liu, Y., Peng, Y., Dai, P., Du, Q., Mei, L., & Xiong, W. (2012). Differential regulation of myosin X movements by its cargos, DCC and neogenin. Journal of Cell Science, 125, 751-762. doi:10.1242/jcs.094946

Lodish, H. F., & Darnell, J. E. (1995). Molecular cell biology / harvey lodish ... [et al.] New York : Scientific American Books : Distributed by W.H. Freeman and Co., c1995; 3rd ed. Retrieved from https://search-ebscohost-com.libez.lib.georgiasouthern.edu/login.aspx?direct=true&db=cat00674a&AN=gsu.573234&site=eds-live

Lu, Q., Ye, F., Wei, Z. Y., Wen, Z. L., & Zhang, M. J. (2012). Antiparallel coiled-coil-mediated dimerization of myosin X Retrieved from https://search-ebscohost-com.libez.lib.georgiasouthern.edu/login.aspx?direct=true&db=edswsc&AN=000311147800024&site=eds-live

Luo, R., An, M., Arduini, BL., & Henion, PD. (2001) Specific pan-neural crest expression of zebrafish Crestin throughout embryonic development. Dev Dyn. 2001 Feb; 220(2): 169-74.

Lumsden, A., & Keynes, R. (1989). Segmental patterns of neuronal development in the chick hindbrain. Nature, (6206), 424. Retrieved from https://search-ebscohost-com.libez.lib.georgiasouthern.edu/login.aspx?direct=true&db=edsgao&AN=edsgcl.7019756&site=eds-live

Luo, R., An, M., Arduini, B. L., & Henion, P. D. (2001). Specific pan-neural crest expression of zebrafish crestin throughout embryonic development. Developmental Dynamics: An Official Publication of the American Association of Anatomists, 220(2), 169-174. Retrieved from https://search-ebscohost-com.libez.lib.georgiasouthern.edu/login.aspx?direct=true&db=cmedm&AN=11169850&site=eds-live

MacDonald, R. B., Debiais-Thibaud, M., Talbot, J. C., & Ekker, M. (2010). The relationship between dlx and gad1 expression indicates highly conserved genetic pathways in the zebrafish forebrain. Developmental Dynamics: An Official Publication of the American Association of Anatomists, 239(8), 2298-2306. doi:10.1002/dvdy.22365

Marín, F., & Puelles, L. (1995). Morphological fate of rhombomeres in quail/chick chimeras: A segmental analysis of hindbrain nuclei. European Journal of Neuroscience, 7(8), 1714-1738. doi:10.1111/j.1460-9568.1995.tb00693.x

Matt N, Ghyselinck NB, Wendling O, Chambon P, Mark M. (2003). Retinoic acid induced developmental defects are mediated by RARbeta/RXR heterodimers in the pharyngeal endoderm. Development 130: 2083–2093.

Mattila, P. K. L., Pekka. (2008). Filopodia: Molecular architecture and cellular functions. Nature Reviews Molecular Cell Biology, 9(6), 446. doi:10.1038/nrm2406

Mattila, P. K., & Lappalainen, P. (2008). Filopodia: Molecular architecture and cellular functions. Nature Reviews Molecular Cell Biology, 9(6), 446. doi:10.1038/nrm2406

McLennan, R., & Kulesa, P. M. (2007). In vivo analysis reveals a critical role for neuropilin-1 in cranial neural crest cell migration in chick. Developmental Biology, 301(1), 227-239. Retrieved from https://search-ebscohost-com.libez.lib.georgiasouthern.edu/login.aspx?direct=true&db=cmedm&AN=16959234&site=eds-live

Minoux, M., & Rijli, F. M. (2010). Molecular mechanisms of cranial neural crest cell migration and patterning in craniofacial development. Development (Cambridge, England), 137(16), 2605-2621. doi:10.1242/dev.040048

Mishina, Y., & Snider, T. N. (2014). Neural crest cell signaling pathways critical to cranial bone development and pathology. Experimental Cell Research, Retrieved from https://search-ebscohost-com.libez.lib.georgiasouthern.edu/login.aspx?direct=true&db=cmedm&AN=24509233&site=eds-live

Mofrad, M., & Kamm, R. (2006). Cytoskeletal mechanics: MODELS AND MEASUREMENTS. Cambridge University Press

Mohler, J. (1988). Requirements for hedgehog, a Segmental Polarity Gene, in Patterning Larval and Adult Cuticle of Drosophila". Genetics 120 (4): 1061–72. PMC 1203569. PMID 3147217

Monsoro-Burq AH, Fletcher RB, Harland RM (2003). Neural crest induction by paraxial mesoderm in Xenopus embryos requires FGF signals. Development 130: 3111–3124.

Monsoro-Burq AH, Wang E, Harland R (2005). Msx1 and Pax3 cooperate to mediate FGF8 and WNT signals during Xenopus neural crest induction. Dev Cell 8: 167–178.

Murone, M., Rosenthal, A. and de Sauvage, F. J. (1999). Hedgehog signal transduction: from flies to vertebrates. Exp. Cell Res. 253, 25-33.

Nakagawa, H., Miki, H., Nozumi, M., Takenawa, T., Miyamoto, S., Wehland, J., et al. (2003). IRSp53 is colocalised with WAVE2 at the tips of protruding lamellipodia and filopodia independently of mena. Journal of Cell Science, 116, 2577-2583. Retrieved from https://search.ebscohost.com/login.aspx?direct=true&db=mnh&AN=12734400&site=eds-live

Nie, S., Kee, Y., & Bronner-Fraser, M. (2009). Myosin-X is critical for migratory ability of xenopus cranial neural crest cells. Developmental Biology, (1), 132. doi:10.1016/j.ydbio.2009.08.018

Niederreither K, Vermot J, Le Roux I, Schuhbaur B, Chambon P, Dolle P. (2003). The regional pattern of retinoic acid synthesis by RALDH2 is essential for the development of posterior pharyngeal arches and the enteric nervous system. Development 130:2525–2534.

Noden D.M. (1983). The role of the neural crest in patterning of avian cranial skeletal, connective, and muscle tissues. Developmental Biology, Retrieved from https://search-ebscohost-com.libez.lib.georgiasouthern.edu/login.aspx?direct=true&db=edsagr&AN=edsagr.US19840017576&site=eds-live

Pi, X., Ren, R., Kelley, R., Zhang, C., Moser, M., Bohil, A. B., et al. (2007). Sequential roles for myosin-X in BMP6-dependent filopodial extension, migration, and activation of BMP receptors Rockefeller University Press. Retrieved from https://search.ebscohost.com/login.aspx?direct=true&db=edsjsr&AN=edsjsr.30050143&site=eds-live

Piotrowski, T., Schilling, T. F., Brand, M., Jiang, Y. J., Heisenberg, C. P., Beuchle, D., et al. (1996). Jaw and branchial arch mutants in zebrafish II: Anterior arches and cartilage differentiation. Development (Cambridge, England), 123, 345-356. Retrieved from https://search.ebscohost.com/login.aspx?direct=true&db=mnh&AN=9007254&site=eds-live

Platt, J. B. (1893). Ectodermic origin of the cartilages of the head: Issues. Anat. Anz., 8, 506-509.

Pomeranz, H. D., Rothman, T. P., & Gershon, M. D. (1991). Colonization of the post-umbilical bowel by cells derived from the sacral neural crest: Direct tracing of cell migration using an intercalating probe and a replication-deficient retrovirus. Development (Cambridge, England), 111(3), 647-655. Retrieved from https://search-ebscohost-com.libez.lib.georgiasouthern.edu/login.aspx?direct=true&db=cmedm&AN=1879333&site=eds-live

Richards, T. A., & Cavalier-Smith, T. (2005). Myosin domain evolution and the primary divergence of eukaryotes. Nature, 436(7054), 1113-1118. doi:10.1038/nature03949

Ridley, A. J., Schwartz, M. A., Burridge, K., Firtel, R. A., Ginsberg, M. H., Borisy, G., et al. (2003). Cell migration: Integrating signals from front to back American Association for the Advancement of Science. Retrieved from https://search.ebscohost.com/login.aspx?direct=true&db=edsjsr&AN=edsjsr.3835875&site=eds-live

Rhinn, M., & Dolle, P. (2012). Retinoic acid signalling during development. Development 139, 843-858 (2012) doi:10.1242/dev.065938

Sasai, N., Mizuseki, K., & Sasai, Y. (2001). Requirement of FoxD3-class signaling for neural crest determination in xenopus. Development (Cambridge, England), 128(13), 2525-2536. Retrieved from https://search-ebscohost-com.libez.lib.georgiasouthern.edu/login.aspx?direct=true&db=cmedm&AN=11493569&site=eds-live

Scambler PJ. 2000. The 22q11 deletion syndromes. Hum Mol Genet 9:2421– 2426.

Schilling, T. F. (1997). Genetic analysis of craniofacial development in the vertebrate embryo. Bioessays, (6), 459. Retrieved from https://search-ebscohost-com.libez.lib.georgiasouthern.edu/login.aspx?direct=true&db=edsgao&AN=edsgcl.19661738&site=eds-live

Selleck, M. A., García-Castro, ,M.I., Artinger, K. B., & Bronner-Fraser, M. (1998). Effects of shh and noggin on neural crest formation demonstrate that BMP is required in the neural tube but not ectoderm. Development (Cambridge, England), 125(24), 4919-4930. Retrieved from https://search-ebscohost-com.libez.lib.georgiasouthern.edu/login.aspx?direct=true&db=cmedm&AN=9811576&site=eds-live

Sittaramane, V., & Chandrasekhar, A. (2008). Expression of unconventional myosin genes during neuronal development in zebrafish. Gene Expression Patterns, (3), 161. doi:10.1016/j.gep.2007.10.010

Spears, R. and Svoboda, K., (2005). Growth Factors and Signaling Proteins in Craniofacial Development. doi:10.1053/j.sodo.2005.07.003

Sokac, A. M., & Bement, W. M. (2000). Regulation and expression of metazoan unconventional myosins. International Review of Cytology, 200, 197-304. Retrieved from https://search-ebscohost-com.libez.lib.georgiasouthern.edu/login.aspx?direct=true&db=cmedm&AN=10965469&site=eds-live

Solc, C.K. et al. (1994) Molecular cloning of myosins from the bullfrog saccular macula: a candidate for the hair cell adaptation motor. Aud. Neurosci. 1, 63–75

Sousa, A. D., & Cheney, R. E. (2005). Myosin-X: A molecular motor at the cell's fingertips. Trends in Cell Biology, (10), 533. doi:10.1016/j.tcb.2005.08.006

Tada, M., Concha, M.L., Heisenberg, C.P., (2002). Non-canonical Wnt signaling and regulation of gastrulation movements. Semin. CellDev. Biol.13, 251–260.

Tapadia, M. D., Cordero, D. R., & Helms, J. A. (2005). It's all in your head: New insights into craniofacial development and deformation. Journal of Anatomy, 207(5), 461-477. doi:10.1111/j.1469-7580.2005.00484.x

Thisse, B., Pflumio, S., Fürthauer, M., Loppin, B., Heyer, V., Degrave, A., et al. (2001). Expression of the zebrafish genome during embryogenesis. ZFIN Direct Data Submission, , (http://zfin.org).

Tickle, C., & Trinkaus, J. P. (1976). Observations on nudging cells in culture. Nature, 261(5559), 413-413. Retrieved from https://search-ebscohost-com.libez.lib.georgiasouthern.edu/login.aspx?direct=true&db=cmedm&AN=934272&site=eds-live

Tokuo, H., & Ikebe, M. (2004). Myosin X transports Mena/VASP to the tip of filopodia. Biochemical and Biophysical Research Communications, 319, 214-220. doi:10.1016/j.bbrc.2004.04.167

Tokuo, H., Mabuchi, K., & Ikebe, M. (2007). The motor activity of myosin-X promotes actin fiber convergence at the cell periphery to initiate filopodia formation. The Journal of Cell Biology, 179(2), 229-238. Retrieved from https://search-ebscohost-com.libez.lib.georgiasouthern.edu/login.aspx?direct=true&db=mnh&AN=17954606&site=eds-live

Trainor, P.A., Ariza-McNaughton, L., Krumlauf, R., 2002. Role of the isthmus and FGFs in resolving the paradox of neural crest plasticity and prepatterning. Science 295, 1288–1291.

Trainor, P. A. (2010). Craniofacial birth defects: The role of neural crest cells in the etiology and pathogenesis of treacher collins syndrome and the potential for prevention Retrieved from https://search-ebscohost-com.libez.lib.georgiasouthern.edu/login.aspx?direct=true&db=edswsc&AN=000285251800007&site=eds-live

Tsui, H.C. et al. (1985) Differentiation of neuronal growth cones: specialization of filopodial tips for adhesive interactions. Proc. Natl. Acad. Sci. U. S. A. 82, 8256–8260

Vaage, S. (1969). The segmentation of the primitive neural tube in chick embryos. with 92 figures Berlin, Heidelberg, New York, Springer, 1969. Retrieved from https://search-ebscohost-com.libez.lib.georgiasouthern.edu/login.aspx?direct=true&db=edshlc&AN=edshlc.000687178-X&site=eds-live

Vickaryous, M. K., & Hall, B. K. (2006). Human cell type diversity, evolution, development, and classification with special reference to cells derived from the neural crest. Biological Reviews, 81(3), 425-455. doi:10.1017/S1464793106007068

Walker, M. B., & Kimmel, C. (2007). A two-color acid-free cartilage and bone stain for zebrafish larvae. Biotechnic & Histochemistry, 82(1), 23-28. doi:10.1080/10520290701333558

Walsh, J. & Mason, I. (2002) Fgf signalling is required for formation of cartilage in the head. Developmental Biology 264 (2003) 522–536 doi:10.1016/j.ydbio.2003.08.010

Wang, W., Melville, D. B., Montero-Balaguer, M., Hatzopoulos, A. K., & Knapik, E. W. (2011). Tfap2a and Foxd3 regulate early steps in the development of the neural crest progenitor population. Developmental Biology, 360(1), 173-185. doi:http://dx.doi.org.libez.lib.georgiasouthern.edu/10.1016/j.ydbio.2011.09.019

Wei, Z., Yan, J., Lu, Q., Pan, L., Zhang, M., & Cheney, R. E. (2010). Cargo recognition mechanism of myosin X revealed by the structure of its tail MyTH4-FERM tandem in complex with the DCC P3 domain National Academy of Sciences. doi:10.1073/pnas.1016567108

Westerfield, M. (2007). THE ZEBRAFISH BOOK: A guide for the laboratory use of zebrafish danio* (brachydanio) rerio (4th ed.). 5274 University of Oregon, Eugene, OR 97403 USA: Univ. of Oregon Press.

Wicki, A., Lehembre, F., Wick, N., Hantusch, B., Kerjaschki, D., & Christofori, G. (2006). Article: Tumor invasion in the absence of epithelial-mesenchymal transition: Podoplanin-mediated remodeling of the actin cytoskeleton. Cancer Cell, 9, 261-272. doi:10.1016/j.ccr.2006.03.010

Wilkie, A. O., & Morriss-Kay, G. (2001). Genetics of craniofacial development and malformation. Nature Reviews.Genetics, 2(6), 458-468. Retrieved from https://search-ebscohost-com.libez.lib.georgiasouthern.edu/login.aspx?direct=true&db=mnh&AN=11389462&site=eds-live

Yelick, P. C., & Schilling, T. F. (2002). Molecular dissection of craniofacial development using zebrafish. Critical Reviews in Oral Biology and Medicine: An Official Publication of the American Association of Oral Biologists, 13(4), 308-322. Retrieved from https://search.ebscohost.com/login.aspx?direct=true&db=mnh&AN=12191958&site=eds-live

Zhu, C., Zheng, Y., & Jia, Y. (2007). A theoretical study on activation of transcription factor modulated by intracellular Ca2+ oscillations. Biophysical Chemistry, 129, 49-55. doi:10.1016/j.bpc.2007.05.006